Programa de Pós-Graduação em
Ciências Mecânicas
Brasília - DF, agosto de 2020

Laboratório de Energia e Ambiente
Energy and Environment Laboratory

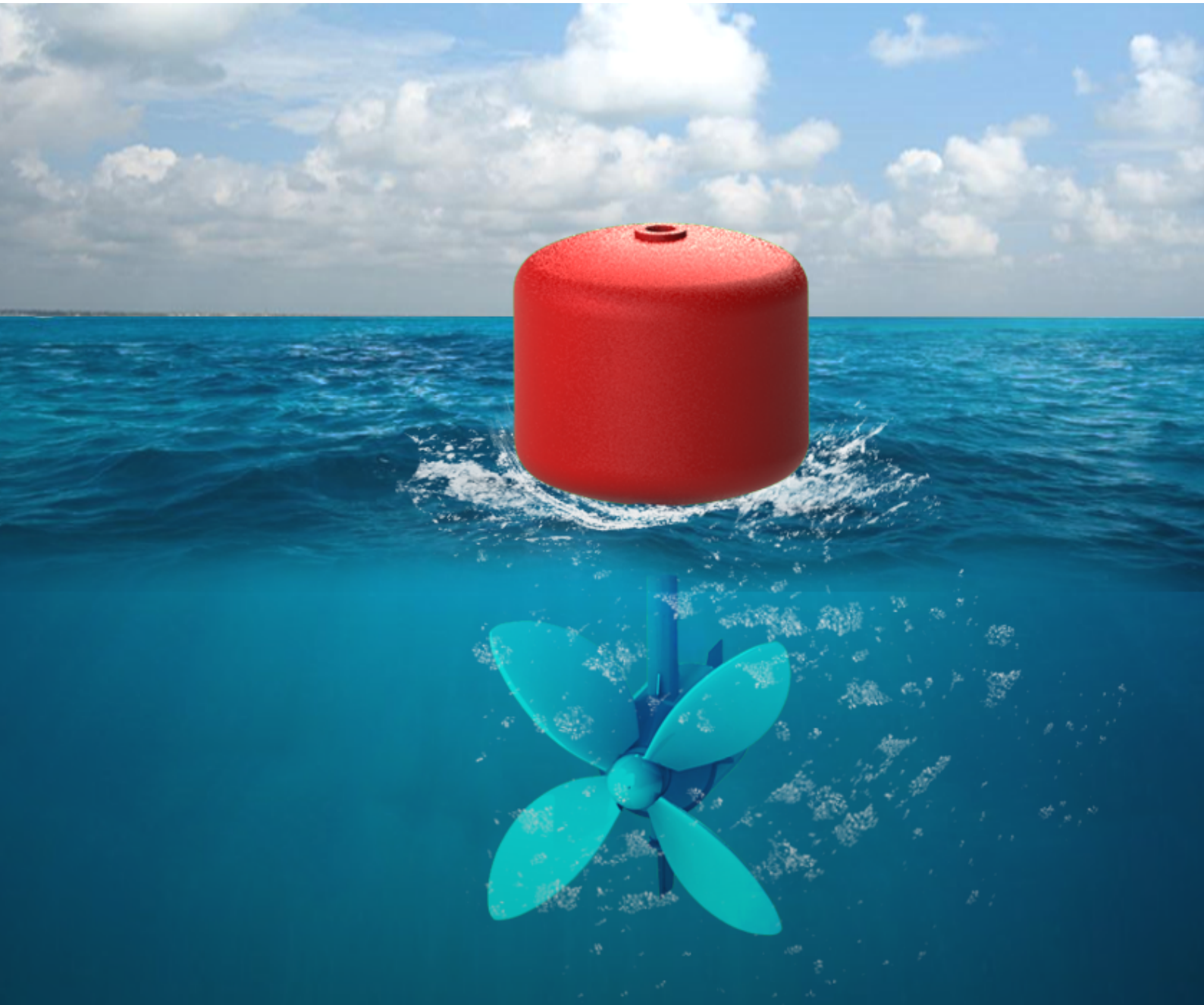

Performance analysis of diffuser-augmented horizontal-axis turbines

Matheus Montenegro Nunes

Matheus Montenegro Nunes
Performance analysis of diffuser-augmented horizontal-axis turbines./ Matheus Montenegro Nunes. – Brasilia - DF, Brasil, August 29, 2020-
105 p. : il. (em cores) ; 30 cm.

Supervisor: Taygoara Felamingo de Oliveira

Tese (Mestrado) – University of Brasilia - UnB
Faculty of Technology
Masters Dissertation, August 29, 2020.

1. Performance analysis 2. Diffuser-augmented turbines 2. Renewable energy I. Taygoara Felamingo de Oliveira II. Universidade de Brasília III. Faculdade de Tecnologia IV. Performance analysis of diffuser-augmented horizontal-axis turbines.

Matheus Montenegro Nunes

Performance analysis of diffuser-augmented horizontal-axis turbines.

A thesis presented to the Faculty of Technology of University of Brasilia in partial fulfillment of the requirements for the degree of

Master of Mechanical Sciences.

Brasilia - DF, Brasil, August 29, 2020:

Taygoara Felamingo de Oliveira
Research Advisor

Antonio Cesar Pinho Brasil Junior
Internal Examiner

Jerson Rogério Pinheiro Vaz
External Examiner

Brasilia - DF, Brasil
August 29, 2020

Let’s be happy.

Agradecimentos

Minha eterna gratidão aos meus pais e ao meu irmão por sempre me amarem e me estruturarem para que eu possa ter essa mentalidade que tenho hoje. Painho, agradeço muito por ser realista na minha vida quando eu parei de ser para mim mesmo. Mainha, agradeço muito por sempre cuidar da gente e de si mesma. Neném, agradeço muito por suas massagens incríveis nos melhores momentos e por ser um irmão maneiro. Minha gratidão por existirem.

Agradeço também a toda a minha família, por estarem presentes sempre quando necessário como um suporte caso algo dê errado conosco.

Agradeço ao meu orientador, professor Taygoara, por procurar sempre o melhor para seus alunos.

Agradeço aos colegas do LEA-UnB, muito especialmente ao Rafael, por ter me inserido nesta oportunidade, me guiando e ajudando em todos os momentos.

Agradeço a UnB, por me proporcionar mais uma etapa memorável da minha vida, e a Coordenação de Aperfeiçoamento de Pessoal de Nível Superior (CAPES) pelo suporte através da bolsa de estudos.

Agradeço a Anne e a Ju, por serem maravilhosas e presentes na minha vida. Ter pessoas que posso chamar de amigas é incrível.

Agradeço a todos os forrozeiros, tangueiros, zoukeiros e todos os outros que estiveram dançando comigo nesta jornada, especialmente aos encontros memoráveis na casa da Vicky. Sem vocês minha vida de UnB não teria sido tão sensacional, eu não saberia nem o quanto estaria perdendo.

Agradeço pelo que tenho hoje e espero continuar agradecendo a todos nessa lista e mais no futuro de minha carreira e vida.

Abstract

A performance analysis of the literature of diffuser-augmented horizontal-axis turbines is presented. A collection of 155 articles in the area is analyzed and classified. The work sample is divided into 16 main research branches for discussion. Power assessment metrics are proposed based on power coefficient and tip-speed-ratio, to quantify and compare all diffuser-augmented turbines in a unified, meaningful manner. Design suggestions for the development of diffuser-augmented turbines are pointed out based on the analysis of 73 cases. A power coefficient assessment on the work sample presented that, in 58% of the cases, the diffuser-augmented turbines surpassed the power coefficient of scaled bare turbines of the same diameter. A tip-speed-ratio assessment presented that almost 90% of the diffuser-augmented turbines developed a narrower operational interval. Five high-performing diffuser-augmented turbines are discussed, highlighting their methodologies and contributions. Caution is advised when coupling a diffuser to a bare turbine with an already high power coefficient; the diffuser-augmented turbine, especially in those cases, should be designed employing a simultaneous diffuser-rotor optimization.

Keywords: Performance Analysis. Systematic analysis. Diffuser-augmented turbines. Wind turbines. Hydrokinetic turbines. Tidal turbines. Renewable energy. Horizontal-axis turbines. Power coefficient.

Resumo

O trabalho apresenta uma análise do desempenho de turbinas de eixo horizontal equipadas com difusores. Um conjunto de 155 artigos na área é analisado e classificado. A amostra de trabalho é dividida entre as 16 principais linhas de pesquisa para discussão. Métricas de análise de desempenho são propostas baseadas em coeficiente de potência e velocidade de ponta de pá, para quatificar e comparar todas as turbinas de eixo horizontal com difusor em uma métrica unificada. Sugestões de projeto para o desenvolvimento de um difusor para turbinas de eixo horizontal são apresentadas com base na análise de 73 casos. A análise de coeficiente de potência sobre a amostra apresenta que, em 58% dos casos, as turbinas com difusor apresentaram um coeficiente de potência maior que a turbina sem difusor ampliada para o mesmo diâmetro. A análise sobre a velocidade de ponta de pá mostra que em quase 90% dos casos as turbinas apresentaram uma diminuição no seu intervalo operacional após a adição do difusor. Cinco turbinas de alto desempenho são discutidas, realçando suas metodologias e contribuições. Cuidado é necessário ao utilizar difusores com turbinas de alto desempenho; especialmente nesses casos, o conjunto turbina-difusor deve ser projetado simultâneamente levando em consideração que vão operar juntos.

Palavras-chave: Análise de desempenho. Análise sistemática. Turbinas com difusor. Turbinas eólicas. Turbinas hidrocinéticas. Turbinas de maré. Energia renovável. Turbinas de eixo horizontal. Coeficiente de potência.

List of Figures

Figure 3.1 – Publication trends. (a) Distribution of work sample by type. (b) Journals with most articles published in the field, along with their CiteScore in 2018. 20
Figure 3.2 – Number of published works on diffuser-enhanced horizontal-axis turbines per year from 1970 to 2020. 21
Figure 3.3 – Change of research groups after 2010 based on co-authorship analysis, highlighting groups whom remained and those who changed. (a) Research groups between 2000 and 2010. (b) Research groups between 2011 and 2014. Made with VOSviewer [148]. 22
Figure 3.4 – Authors with most works published on diffuser-enhanced turbines, with added time period in which those publications occurred. 23
Figure 3.5 – Number of occurrences of main author keywords on three time periods. 26
Figure 4.1 – Illustration of parameters on a diffuser-augmented turbine; cross-section view. 27
Figure 5.1 – Characteristics of conical and airfoil-shaped diffusers in cross-section views. Conical diffuser in (a) and airfoil-shaped diffuser in (b). Illustration of conical and airfoil-shaped diffuser velocity distributions in (c) and (d). 35
Figure 5.2 – Illustration of building-augmented horizontal-axis turbines. Bahrain Towers on (a) and The Strata on (b). 38
Figure 5.3 – Characteristics of curved diffuser in cross-section views. Airfoil-shaped diffuser in (a) and curved diffuser in (b). Illustration of airfoil-shaped and curved diffuser velocity profiles in (c) and (d), with detail to the recirculation zone that makes the curve shape hydrodynamic-similar to an airfoil profile; reused and edited with permission [41]. 40

Figure 5.4 – Illustration of flange aspects in cross-section views. Detail to flange on curved diffuser in (a). Illustration of velocity field and recirculation zones from axisymmetric numerical analysis in (b), reused and edited with permission [78]. Particle-image velocimetry of recirculation zones in (c), reused with permission [25]. 42
Figure 5.5 – Illustration of control plates on diffuser, reused with permission [108]. 44
Figure 5.6 – Lobed diffusers viewed from the back. Scheme in (a), reused and edited with permission [57]. Lobed diffuser by FloDesign, in (b), courtesy of Ewan O'Sullivan [123]. 45
Figure 5.7 – Illustration of vortex generators on diffuser-augmented turbine [144]. 46
Figure 5.8 – Detail to frontal nozzles in cross-section view of diffuser-augmented turbines. Frontal nozzles in: airfoil-shaped diffuser in (a), curved diffuser in (b), conical diffuser in (c). 47
Figure 5.9 – Multi-slots diffusers. Cross-section view in (a). Commercial design by FloDesign, in (b) [71, 56]. 48
Figure 5.10–Illustration of five diffuser-augmented turbine's arrangement, with detail to Multi-turbine system's gap parameter. Distinction of two and three turbine's arrangement. 49
Figure 5.11–Alternative turbine arrangement proposed for research. 50
Figure 5.12–Illustration of diffuser-augmented twin-rotor turbine, and its counter-rotating aspect. 52
Figure 6.1 – Power coefficient comparison between diffuser-augmented turbine and bare turbine. Comparison on usual C_p metric in (a). Comparison on proposed E_d metric in (b). 56
Figure 6.2 – TSR_{width} and TSR_{center} illustration on a power coefficient curve. Data obtained from previous work [104]. 57
Figure 7.1 – Distribution of diffuser-augmented turbines found on the literature based on power coefficient. (a) Based on C_p metric. (b) Based on C_p^d metric. 60
Figure 7.2 – Distribution of diffuser-augmented turbines found on the literature based on E_d. 61

Figure 7.3 – Influence of diffuser on TSR. Comparison of changes between bare turbine and diffuser-augmented turbine. Two design points of interest are highlighted. 62
Figure 7.4 – Dispersion of the diffuser-augmented turbines respective to C_p^d and A_d/A_r. Five design points of interest are highlighted. 64
Figure 7.5 – Diffuser-augmented turbine optimization. Analyzed cases in (a), with objectively best ones in black. Selected profile H illustration in (b), referred as design point 2. Reused and edited with permission [78] . 67
Figure 7.6 – Diffuser-augmented turbine with flange inclination. Flange with positive 10° angle in (a), referred design point 3, and 0° angle in (b). Reused and edited with permission [59]. 67
Figure 7.7 – Several diffuser-augmented turbines with varying lengths, experiments made with the same rotor [105]. Diffuser $C0$ - $0.100L/D_r$ in (a), Ci - $0.137L/D_r$ in (b), Cii - $0.221L/D_r$ in (c), $Ciii$ - $0.371L/D_r$ in (d). 68
Figure 7.8 – Relation between the diffuser-enhancement achieved, E_d, and the power coefficient, C_p^b, of their respective bare turbines. Three areas of interest are highlighted. 69
Figure 7.9 – Conical diffuser-augmented turbine by Kosasih and Saleh [83]. . . . 70
Figure A.1 – Keywords for advanced search in Scopus database. 96

List of Tables

Table 2.1 – Summary of database search keywords. 19
Table 3.1 – Most cited works on diffuser enhanced turbines 24
Table 3.2 – Most cited recent works on diffuser enhanced turbines, from 2010 to 2020. 25
Table 5.1 – Research branches of interest with their respective reference page. . . 30
Table 7.1 – Common traits of a low and high standard diffusers. 65
Table B.1 – Power coefficient and tip-speed ratio data of diffuser-augmented turbines - Part I 98
Table B.2 – Power coefficient and tip-speed ratio data of diffuser-augmented turbines - Part II 99
Table B.3 – Power coefficient and tip-speed ratio data of diffuser-augmented turbines - Part III 100
Table B.4 – Power coefficient and tip-speed ratio data of diffuser-augmented turbines - Part IV 101
Table C.1 – Geometry data of diffuser-augmented turbines - Part I 102
Table C.2 – Geometry data of diffuser-augmented turbines - Part II 103
Table C.3 – Geometry data of diffuser-augmented turbines - Part III 104
Table C.4 – Geometry data of diffuser-augmented turbines - Part IV 105

Nomenclature

Geometry

A_d	Diffuser's maximum cross-sectional area	m^2
A_i	Diffuser's inlet area	m^2
A_r	Rotor's spanning area	m^2
D_d	Diffuser's maximum diameter	m
D_i	Diffuser's inlet diameter	m
D_r	Rotor's diameter	m
L_n	Nozzle's length	m
L_e	Diffuser's expansion length	m
L	Total diffuser length	m
s	Multi-turbine system's gap	m
θ	Diffuser's expansion angle	$^\circ$

Performance and flow

C_p^b	Bare turbine's power coefficient	-
C_p	Diffuser-augmented turbine's power coefficient	-
C_p^d	Diffuser-augmented turbine's actual power coefficient	-
E_d	Diffuser enhancement	-
P_{bare}	Power generated by bare turbine	W
$P_{diffuser}$	Power generated by diffuser-augmented turbine	W

TSR	Tip-speed-ratio	-
U	Unperturbed flow's mean speed	m/s
u	Flow's axial velocity	-
ω	Rotor's angular speed	rad/s
ρ	Fluid density	kg/m^3

Contents

1 INTRODUCTION 17

2 SOURCE MINING 18

3 BIBLIOMETRIC DATA 20

4 PARAMETERS INTRODUCTION 27

5 RESEARCH BRANCHES 30
5.1 Theoretical framework 30
5.1.1 Analytical models 31
5.1.2 Semi-analytical models 32
5.2 Acoustics 33
5.3 Airfoil-shaped diffuser 34
5.3.1 Influence of the airfoil shape on the power coefficient 35
5.3.2 Influence of the airfoil shape on the pressure distribution 36
5.3.3 Influence of the airfoil shape on the axial velocity distribution . . . 36
5.3.4 Optimization of the airfoil profile 36
5.4 Blade-tip effects 36
5.5 Building-augmented wind turbines 37
5.6 Curved diffuser 39
5.7 Diffuser length 41
5.8 Flanges 42
5.9 Flow mixers 43
5.9.1 Control plates 44
5.9.2 Lobed diffusers 45
5.9.3 Vortex generators 46
5.10 Frontal nozzles 46
5.11 Multi-slots 47
5.12 Multi-turbine system 49

5.13 Simultaneous diffuser-rotor design 50
5.14 Twin-rotors on diffusers 51
5.15 Yaw and shear flow effects 52
5.16 Other diffuser concepts 53

6 METRICS OF ASSESSMENT 54
6.1 Power coefficient metrics 54
6.2 Tip-speed-ratio metrics 56

7 PERFORMANCE ASSESSMENT 59
7.1 Power coefficient distribution 59
7.2 Diffuser influence on tip-speed-ratio 62
7.3 Well designed diffuser-augmented turbines 64
7.4 Diffuser enhancement 68

8 CONCLUSIONS 71

BIBLIOGRAPHY 73

APPENDIX 95

APPENDIX A – DATABASE SEARCH KEYWORDS 96

APPENDIX B – DIFFUSER-AUGMENTED TURBINE'S DATA 98

APPENDIX C – DIFFUSER-AUGMENTED TURBINE'S GEOMETRY 102

1 Introduction

The increased demand for a more renewable energy grid has motivated the development of the research on wind, tidal, and hydrokinetic turbines technology. For long, prevailed the thought that increasing the rotor diameter was the only feasible way to increase the turbine's power output. Disproving that, research on diffuser-augmented turbines has been gaining popularity in recent years as an alternative and promising method. Due to this sudden surge in the area, the literature developed in a non-uniform and spread way.

In recent years, many authors, explored the subject. They classified and provided examples on different types of diffuser-augmented turbines, presenting an idea of the state-of-the-art [5]. Nevertheless, they were mostly concerned about explaining the subject broadly, with several examples of different technologies, lacking a summarized collection approaching all results achieved in the field. More cohesive guidance is needed for ease of finding what was already tested and what research path one should take. The present work uses data from already published works. This data is analyzed to gather results over several different areas that wouldn't be possible otherwise, when performing an analysis of a single article. This macro approach permits the deduction of several unanswered or unverified questions, for example: What are the effects of the diffuser on the turbine's tip-speed-ratio? Which is the better option: increasing the rotor diameter or using a diffuser? What areas are open and interesting for research?

In that manner, the present work provides the following content:

- discussion of the systematic methodology employed in the literature;
- bibliometric data on topic;
- presentation of relevant parameters;
- main research branches and their most important findings;
- performance assessment of diffuser-augmented turbines found in the literature.

2 Source mining

The present work aims to swift through all relevant works published on diffuser-augmented horizontal turbines, or as close as possible to that. From there, it presents all of these works' information in a retraceable form. Further, a study is performed, not only over isolated samples but also over the whole collection of articles gathered.

A systematic approach to the bibliography is adopted. The present chapter summarizes the method, but the interested reader may obtain more information from Cronin et al. [34] and Pagani et al. [117].

The step-by-step method performed is presented below:

- Determination of the research topics and database.
- Selection of proper search keywords and filtering of all relevant data.
- Classification, reading, and analysis of articles.
- Sorting of the gathered data and presentation of findings.

The research topic is defined as "Diffuser-augmented horizontal-axis turbines." Availability and content are two important factors to be considered about the database; different areas will be better evaluated in different databases, with different aims. One can also opt for using more than one database and joining all information together. The primary database of choice here was the Scopus [46]: vast and with an outstanding advanced search engine. It does not limit itself to Elsevier but also contemplates more than 5000 other publishers, a large part of its content coming from Elsevier, Springer, Wiley-Blackwell, Taylor & Francis, and IEEE [45].

Due to the developing nature of the topic, the initial search has to be as broad as possible. The literature of diffuser-augmented turbines often mixes with the one of hydrokinetic turbines, wind turbines, tidal turbines, along with others. Table 2.1 summarizes the keywords employed to perform the search. The full set of keywords are presented in Appendix A, that includes the used wildcards, boolean operators, and

proximity operators. The search resulted in 426 documents on the English language, of which 155 were used in the elaboration of the present work.

Table 2.1 – Summary of database search keywords.

Any of those terms	Along with any of those sets
Diffuser	Hydro, wind, tidal, current or marine turbine
Shroud	Horizontal-axis turbine
Concentrator	Augmented turbine
Ducts	

3 Bibliometric data

Bibliometric data can be compiled from the work sample to show the state of the research in the area. The analysis covers data about co-authorship networks, publishing trends, most relevant journals and word occurrence analysis.

Figure 3.1(a) presents the main publication types in the subject, where 60% are journal articles. Due to the amount of articles published, Figure 3.1(b) highlights the journals with most articles published in the field, along with their CiteScore in 2019.

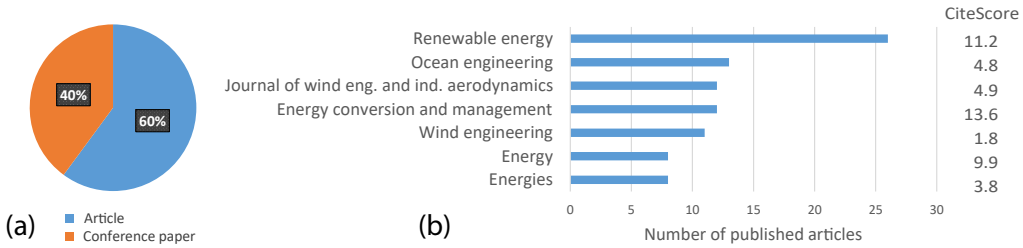

Figure 3.1 – Publication trends. (a) Distribution of work sample by type. (b) Journals with most articles published in the field, along with their CiteScore in 2018.

There is a trend of publications being spread out between different journals. The main published journals consist of only 36% of all journal published articles. No correlation was found between the CiteScore and the number articles published in that specific journal. That information points to the fact that authors tend to seek more fitting journals for their topic. This is evident on Ocean Engineering, with only articles on hydrokinetic and Tidal turbines; Journal of Wind Engineering and Industrial Aerodynamics and Wind Engineering, with most of the recent wind-focused technologies on diffuser-enhanced turbines.

Figure 3.2 introduces how the number of publications on diffuser-enhanced turbines changed through the years. It is noticeable that the area received relatively few attention from researchers until 2010, when its growth began. Works from 1972 to 1991 were mostly from Igra, Foreman, Gilbert and Fletcher, whom have done exhaustive numerical and experimental works on different diffuser designs.

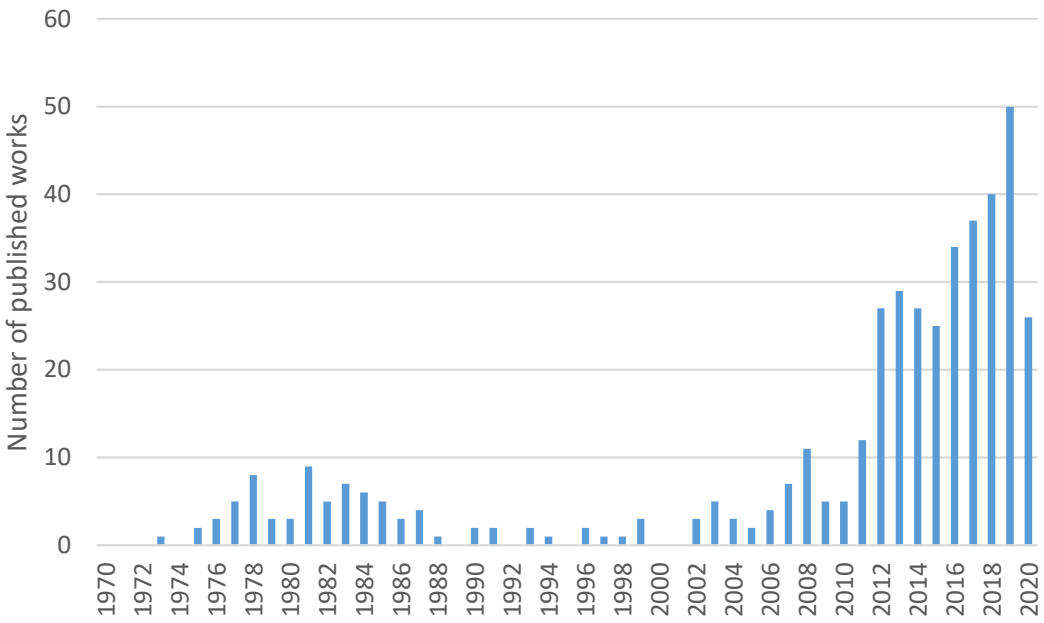

Figure 3.2 – Number of published works on diffuser-enhanced horizontal-axis turbines per year from 1970 to 2020.

The effects of the significant rise in the field after 2010 can be better observed during a co-authorship analysis, done on VOSviewer, software version 1.6.10 [148]. For that, two time intervals will be analyzed: before the rise, between 2000 and 2010, and right after the rise, between 2011 and 2014. In that manner we can observe the immediate implications of this sharp rise in the field.

Figure 3.3 presents an author network on those two time periods: between 2000 and 2010, on Figure 3.3(a), and between 2011 and 2014, on Figure 3.3(b). Each circle size indicates the number of published articles by an author. The connecting lines indicate an article published by the two authors. In Figure 3.3, we can observe different research groups, each of those groups isolated in their respective clusters. The focus point is on how the people working in the area changed between the two time periods.

In the first time period, most of the research papers published on the topic of diffuser-enhanced turbines, are due to the Japanese group working from the Research Institute for Applied Mechanics, in Kyushu University (red network of Ohya et al.).

In the period between 2011 and 2014, despite the most active group still remaining the same, several different research groups, in different countries, have published on diffuser-enhanced turbines. Above that, none of the researchers marked in green, who published between 2000 and 2010, had any publications in the area between 2011 and 2014. Nevertheless, the increase on publications on the field as a whole is evident when comparing the big circles' diameters.

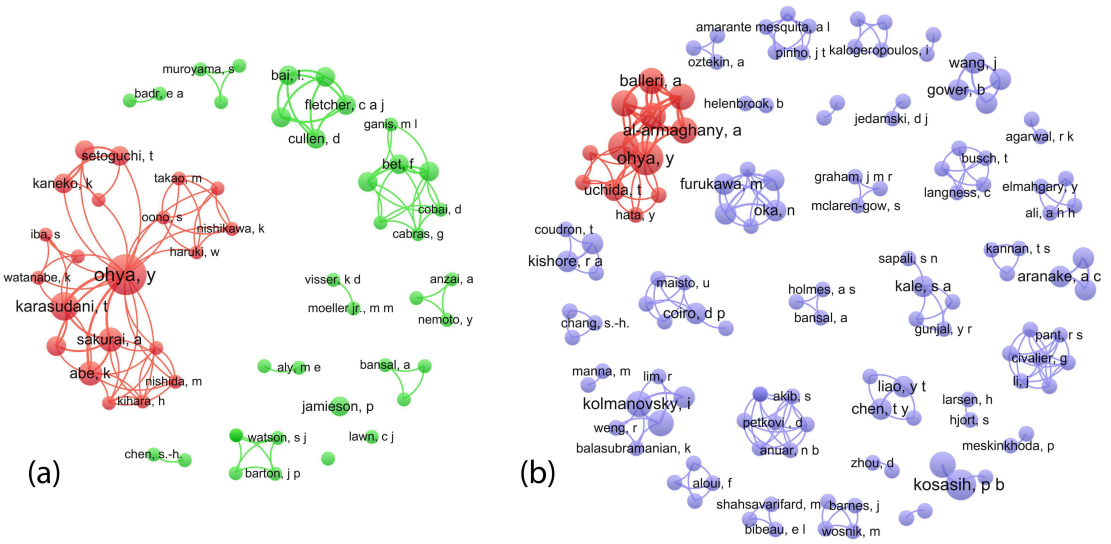

Figure 3.3 – Change of research groups after 2010 based on co-authorship analysis, highlighting groups whom remained and those who changed. (a) Research groups between 2000 and 2010. (b) Research groups between 2011 and 2014. Made with VOSviewer [148].

Another relevant point to present is the main publishing authors in the field. Figure 3.4 summarizes the authors with most publications. As an added reference, the works with most citations published in the field are listed in Table 3.1; the recent works with most citations (from 2010 to 2020) are listed in Table 3.2.

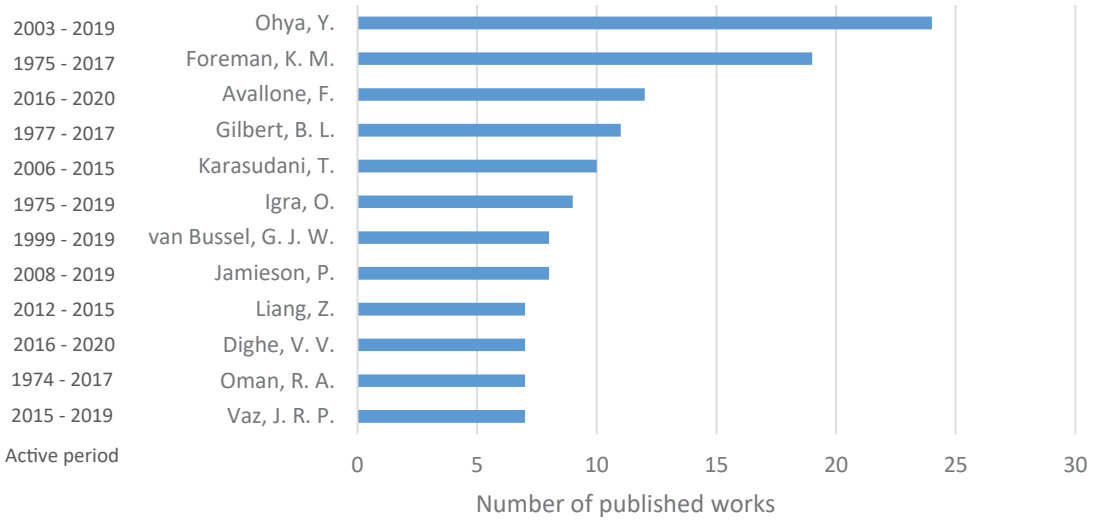

Figure 3.4 – Authors with most works published on diffuser-enhanced turbines, with added time period in which those publications occurred.

Table 3.1 – Most cited works on diffuser enhanced turbines

Authors	Year	Title	Source	#Citations	#Reference
Ohya et al.	2008	Development of a shrouded wind turbine with a flanged diffuser	Journal of Wind Eng. and Ind. Aerodynamics	180	[106]
Ohya and Karasudani	2010	A shrouded wind turbine generating high output power with wind-lens technology	Energies	178	[105]
Abe et al.	2005	Experimental and numerical investigations of flow fields behind a small wind turbine with a flanged diffuser	Journal of Wind Eng. and Ind. Aerodynamics	137	[3]
Igra, O.	1981	Research and development for shrouded wind turbines	Energy Conversion and Management	133	[65]
Van Bussel	2007	The science of making more torque from wind: Diffuser experiments and theory revisited	Journal of Physics: Conference Series	130	[146]
Abe and Ohya	2004	An investigation of flow fields around flanged diffusers using CFD	Journal of Wind Eng. and Ind. Aerodynamics	118	[4]
Gilbert and Foreman	1983	Experiments with a diffuser augmented model wind turbine	Journal of Energy Resources Technology, Transactions of the ASME	100	[51]
Matsushima et al.	2006	Characteristics of a highly efficient propeller type small wind turbine with a diffuser	Renewable energy	82	[97]
Grant et al.	2008	Urban wind energy conversion: The potential of ducted turbines	Renewable energy	77	[1]
Howey et al.	2011	Design and performance of a centimetre-scale shrouded wind turbine for energy harvesting	Smart Materials and Structures	68	[62]
Lawn, C. J.	2003	Optimization of the power output from ducted turbines	Journal of Power and Energy	67	[87]
Foreman et al.	1978	Diffuser augmentation of wind turbines	Solar energy	62	[49]

Table 3.2 – Most cited recent works on diffuser enhanced turbines, from 2010 to 2020.

Authors	Year	Title	Source	#Citations	#Reference
Ohya and Karasudani	2010	A shrouded wind turbine generating high output power with wind-lens technology	Energies	178	[105]
Howey et al.	2011	Design and performance of a centimetre-scale shrouded wind turbine for energy harvesting	Smart Materials and Structures	68	[62]
Gaden et al.	2010	A numerical investigation into the effect of diffusers on the performance of hydro kinetic turbines using a validated momentum source turbine model	Renewable energy	56	[50]
Jafari and Kosasih	2014	Flow analysis of shrouded small wind turbine with a simple frustum diffuser with computational fluid dynamics simulations	Journal of Wind Engineering and Industrial Aerodynamics	54	[67]
Bontempo and Manna	2014	Performance analysis of open and ducted wind turbines	Applied Energy	53	[19]
Kosasih and Tondelli	2012	Experimental study of shrouded micro-wind turbine	Procedia Engineering	48	[81]
Bontempo and Manna	2016	Effects of the duct thrust on the performance of ducted wind turbines	Energy	47	[20]
Vermillion et al.	2014	Model-based plant design and hierarchical control of a prototype lighter-than-air wind energy system, with experimental flight test results	IEEE Transactions on Control Systems Technology	46	[152]
Kishore et al.	2013	Small-scale wind energy portable turbine (SWEPT)	Journal of Wind Engineering and Industrial Aerodynamics	46	[79]
Aranake et al.	2015	Computational analysis of shrouded wind turbine configurations using a 3-dimensional RANS solver	Renewable energy	42	[11]
Vaz et al.	2015	An extension of the Blade Element Momentum method applied to Diffuser Augmented Wind Turbines	Energy Conversion and Management	38	[10]

The results of a word occurrence analysis are shown in Figure 3.5, which brings the most recurrent author-keywords. It is worth to point out an inclination to wind turbines in the area, but also the growing trend in the last years of applying the diffuser technology to hydrokinetic turbines. Some of the most studied designs also appear, such as flanges, airfoils and optical diffusers (An explanation on those will follow on Chapter 5). It can also be noted how the topic of multi-rotor system and design optimization started to grow, while the topic of airfoil design declined.

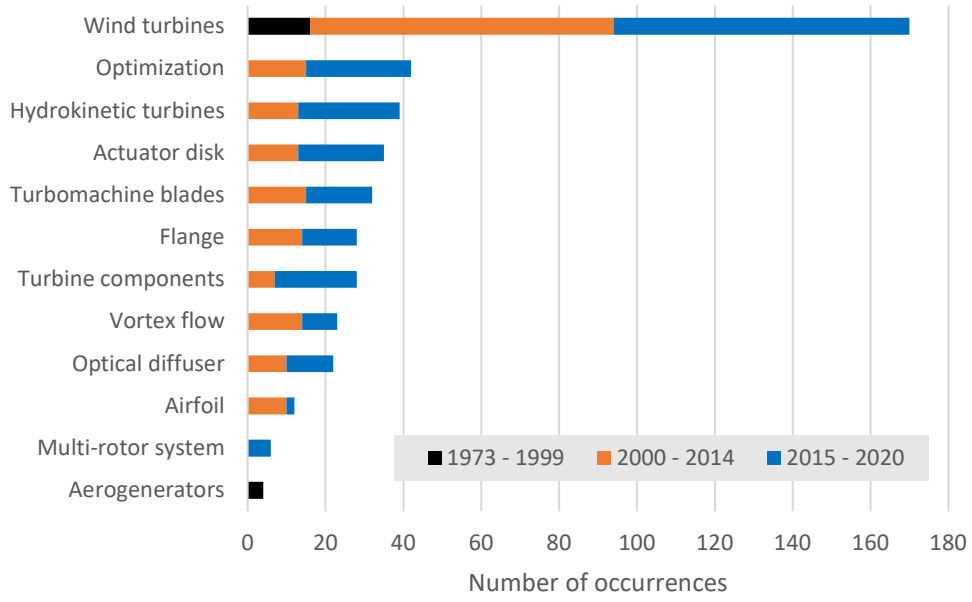

Figure 3.5 – Number of occurrences of main author keywords on three time periods.

4 Parameters introduction

The parameters description is separated into two parts:

- The current chapter—Parameters introduction. The parameters presented are often employed in the literature of diffuser-augmented turbines and referred to in the discussion of the main research branches.
- Chapter 6—Metrics of assessment. Parameters are proposed to analyze the performance of several diffuser-augmented turbines under a unified metric.

To better discuss the results found across several studies, Figure 4.1 illustrates commonly employed parameters on a diffuser-augmented turbine schematic.

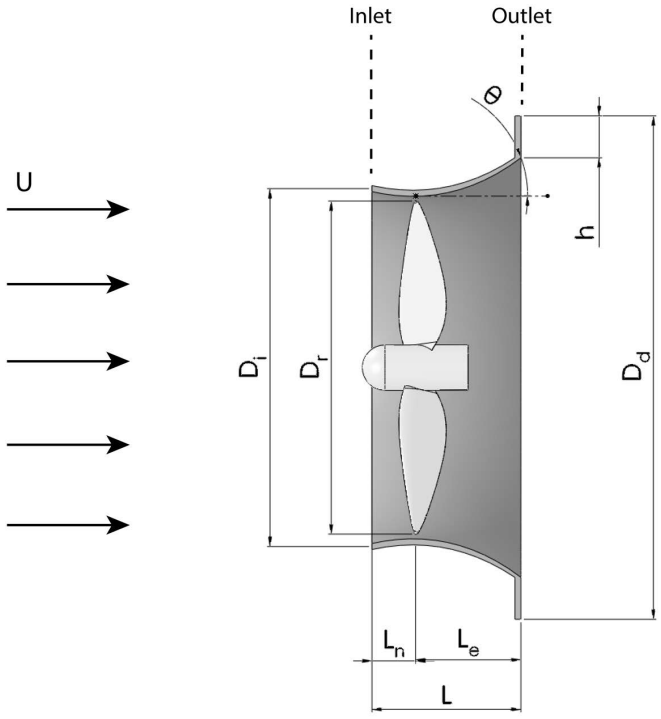

Figure 4.1 – Illustration of parameters on a diffuser-augmented turbine; cross-section view.

Concerning geometry: D stands for diameter, L for total length, L_n for nozzle length, L_e for expansion length, h for flange height, and θ for expansion angle. The equation that describes the relevant areas is defined as

$$A_k = \pi(D_k/2)^2, \tag{4.1}$$

where $k = i, r, d$, standing for inlet, rotor and diffuser's maximum cross-section, respectively.

The flow's axial velocity, u, is the flow's velocity profile at the turbine's centerline; it is parameterized by U, the flow's mean speed. The Multi-turbine system's gap, s, is used when discussing the arrangement of several diffuser-augmented turbines; it represents the distance between two diffusers in the arrangement and will be illustrated further on Section 5.12.

The bare turbine's power coefficient, C_p^b, is the ratio between the power generated by the bare turbine and the power available to it,

$$C_p^b = \frac{P_{bare}}{\frac{1}{2}\rho U^3 A_r}. \tag{4.2}$$

where ρ represents the working fluid's density and U represents the flow's mean speed.

The diffuser-augmented turbine's power coefficient, C_p, is the metric which most authors adopt. It represents the ratio between the power generated by the diffuser-augmented turbine and the power available to the bare turbine,

$$C_p = \frac{P_{diffuser}}{\frac{1}{2}\rho U^3 A_r}. \tag{4.3}$$

The present work proposes an analysis of diffuser-augmented turbines that takes into consideration the diffuser size. To achieve that, the diffuser-augmented turbine's actual power coefficient, C_p^d, is defined. That parameter is the ratio between the power generated by the diffuser-augmented turbine and the power available to the diffuser's area,

$$C_p^d = \frac{P_{diffuser}}{\frac{1}{2}\rho U^3 A_d}. \tag{4.4}$$

The tip-speed-ratio, TSR, is defined as

$$TSR = \frac{\omega R}{U}, \tag{4.5}$$

where ω is the rotor's angular speed and R is the rotor's radius.

The power coefficient and tip-speed-ratio are the two main dimensionless parameters to the study of horizontal-axis turbines. Nonetheless, the full-scale Reynolds number is essential to a complete description of the framework in terms of dimensionless parameters.

The maximum amount of energy that an extraction device in an open flow can gather is quantified as approximately 59.3% of the available energy. This is commonly known as the Betz Limit [17], meaning that a bare turbine would never achieve a C_p^b value higher than 0.593.

Instead of "Betz limit", the term "Betz limit for bare turbines" will be used throughout the present work. The specification is made because, when applied to systems with elements that alter the flow field but do not extract energy themselves, the energy extraction limit is higher than 0.593 [69]. Such systems, for example, are diffuser-augmented turbines. Due to that, each turbine will present a different limit than the established for bare turbines. This information is presented earlier so that the reader does not feel uncomfortable with reported C_p^d values that may seem illogical.

5 Research branches

The presented articles focused on different subjects, all aiming to increase the diffuser-augmented turbine's power coefficient or change its characteristics. Table 5.1 lists some of the most relevant, recent or frequent topics researched. The following sections discuss each one of those entries and the findings in that field.

Table 5.1 – Research branches of interest with their respective reference page.

Topic	Reference page
Theoretical framework	30
Acoustics	33
Airfoil-shaped diffuser	34
Blade-tip effects	36
Building-augmented wind turbines	37
Curved diffuser	39
Diffuser length	41
Flanges	42
Flow mixers	43
Frontal nozzles	46
Multi-slots	47
Multi-turbine system	49
Simultaneous diffuser-rotor design	50
Twin-rotors on diffusers	51
Yaw and shear flow effects	52
Other diffuser concepts	53

5.1 Theoretical framework

The pioneering work on the theoretical aspects of diffuser-augmented turbines is due to Lilley and Rainbird [89]. In 1956, they used the one-dimensional flow theory to evaluate the performance and design of diffuser-augmented turbines, or ducted windmills, as called on the article. They concluded that there is no increase in the power coefficient if the diffuser's exit area is used instead of the rotor's swept area in the C_p definition.

Foreman et al. [49], in 1978, and their other previous works [52, 116], presented a simpler model to be used, in comparison with the one from Lilley and Rainbird. All the authors mentioned above corroborated their models with experimental results.

De Vries [37], in 1979, discussed several concepts for diffusers and the theory behind horizontal-axis wind turbines. He coupled numerical analysis to one-dimensional theory to evaluate the effects of a diffuser around a turbine, not considering wake rotation.

A common feature in models of [89, 49, 52, 116, 37] was the necessity of empirical parameters. Experimental data are necessary to provide information on the parameters for each geometry and situation. Only then it is feasible to predict the diffuser's power coefficient and efficiency parameters.

5.1.1 Analytical models

Jamieson [68, 69], in 2008 and 2009, and Van Bussel et al. [146], in 2007, based themselves on a modified version of the standard actuator disk model [23] to account for the presence of a diffuser influencing the flow field. Those models led to a new limit theory, not constraining themselves to the open-flow case of the Betz limit, showing that diffuser-augmented turbines can reach power coefficients higher than 0.593. Van Bussel et al. [146] developed a model to work only on ideal scenarios to evaluate the performance of diffuser-augmented turbines. Their model assumes continuity between the velocities upstream and downstream of the diffuser, as in conventional wind turbines. That assumption makes the model restricted to compact diffusers. Jamieson [68, 69] included the expansion angle and a factor to account for base pressure at the rotor's zero thrust condition. The diffuser efficiency term was provided for non-ideal systems, considering flow separation, viscous loss, and base pressure variations through the diffuser.

Both articles [146, 68, 69] reported that, in an ideal system, 8/9 would be the optimal loading factor. However, for non-ideal systems, Lawn [87] and Foreman et al. [49] concluded that the optimal loading factor changes based on the loading coefficient, back pressure coefficient, and diffuser performance. The zero-thrust and compact diffuser assumptions are often not desired, and thus semi-analytical models are used to rectify those shortcomings.

5.1.2 Semi-analytical models

Gaden and Bibeau [50], in 2010, proposed a momentum source model and validated it against the Betz theory. They investigated the diffuser size and expansion angle, defining the point that marks the decrease in power production due to the flow separation.

Shives and Crawford [136, 137], in 2011, used the model proposed by Lawn [87] and developed an empirical method to evaluate the performance of diffuser-augmented turbines using RANS-CFD. Khamlaj and Rumpfkeil [77], in 2017, extended on the same model to provide a semi-empirical method that can be used to decide a preliminary design for a diffuser-augmented turbine.

Bontempo and Manna [18, 19, 20], from 2013 to 2016, extended on the non-linear actuator disk theory of Conway [33]. They worked with diffuser-augmented turbines and provided an exact solution for the inviscid axisymmetric flow generated, using a superposition of ring vortices arranged over the diffuser surface and on the wake. They presented a semi-analytical solution to the problem that takes into account the diffuser-rotor non-linear interaction and can handle wake rotation, radial load distributions, and single-body diffuser shapes.

Vaz et al. [43], in 2014, extended on the Blade Element Momentum Method to propose a one-dimensional model that takes into account the blade geometry at low computational costs. Vaz and Wood [149], in 2016, developed a model for rotor optimization considering the diffuser's presence.

Liu and Yoshida [93], in 2015, extended on the generalized actuator disk model proposed by Jamieson [68]. They included the effective diffuser efficiency, Glauert corrections, and established an empirical model to predict the axial velocity profile to include an approximation of the axial velocity at the rotor plane.

Michał et al. [101, 102], in 2016, compared the fully resolved rotor model with the actuator disk model in the rotor design point. They verified the results using experimental tests. The actuator disk model worked as an approximation for rotor-diffuser geometry optimization.

Baratchi et al. [15], in 2019, modified the actuator line method to account for

diffuser-augmented turbines, corroborating the results with experimental tests. The method is based on the so-called projection factor, an ad hoc parameter which has to be calibrated. The same authors [16], in 2020, coupled the blade element method with the actuator disk theory. The method did not capture vortex related phenomena, as expected by the authors, but provided accurate measurements of the diffuser-augmented turbine's power and thrust coefficients.

Bontempo and Manna [21], in 2020, used axial momentum theory to model an ideal diffuser-augmented turbine, taking into account the 2D nature of the flow and the blade-tip gap. Using the model corrections, they also verified the optimum loading factor of 8/9 for a diffuser-augmented turbine. The power coefficient of an actuator disk in a simple convergent-divergent duct was proven to have the same limit as the Betz disk: 16/27, or 0.593. However, for diffuser-augmented turbines, the power coefficient obtained can exceed not only a bare turbine of the same size but also the Betz limit for bare turbines. They found that taking into consideration the effects of blade-tip gaps with 1% of the rotor diameter did not significantly alter the results.

Several other works used the actuator disk model, coupled with a diffuser to evaluate various parameters through numerical analysis and could be used as a reference for the interested reader on further applications of the technique [8, 39, 40, 85, 107, 139, 153].

5.2 Acoustics

Wind turbines are an environmental noise source, and the addition of a diffuser is still an open topic for discussion. The effects of the blade tip vortices and the wide-array of geometries are still to be evaluated.

Hashem et al. [58], in 2017, performed an aero-acoustic computational study to investigate the noise produced by 'Wind-Lens' turbines, referring to the set of experiments performed by Ohya et al. [105] in 2010. They analyzed results in terms of the Overall Sound Pressure Level, OASPL. They reported lower sound pressure for the bare wind turbine, an averaged OASPL of 53 dB, when compared to their diffuser-augmented counterparts, ranging from an averaged OASPL of 62 to 78 dB. The *Ci* shape being the one reported for 62 dB. Those results were measured at a distance of 0.9m.

Avallone et al. [12, 13], in 2019 and 2020, studied the effects of tip-clearance ratio on the aeroacoustics of diffuser-augmented turbines. They reported a strong correlation between tip clearance ratio and the sound pressure on the far-field, reaching up to a 10 dB increase.

Dighe et al. [42], in 2020, made experiments on diffuser-augmented turbines in yawed conditions and measured their sound pressure with a circular array of microphones normal to the plane of rotation. They reported varying sound pressure at different radial points, but no significant difference due to the yawed condition.

Some articles reported noise reduction from the addition of diffuser around a turbine due to the weakening of blade-tip vortices but did not provide measurements [2, 108].

5.3 Airfoil-shaped diffuser

As often thought, the primary way to increase a diffuser's potential is to increase its outlet area. To reduce the diffuser's length and keep the same outlet area, higher expansion angles are employed. A usual problem in this situation is the boundary layer separation from the inner diffuser's surface, due to the high adverse pressure gradients. This phenomenon decreases the diffuser-augmented turbine's power coefficient. A common technique employed, to avoid this separation, is changing the diffuser shape from conical to an airfoil one, as illustrated in the transition of Figures 5.1(a) and 5.1(c) to 5.1(b) and 5.1(d). The following items discuss the main findings on airfoils applied to diffuser-augmented turbines by different authors.

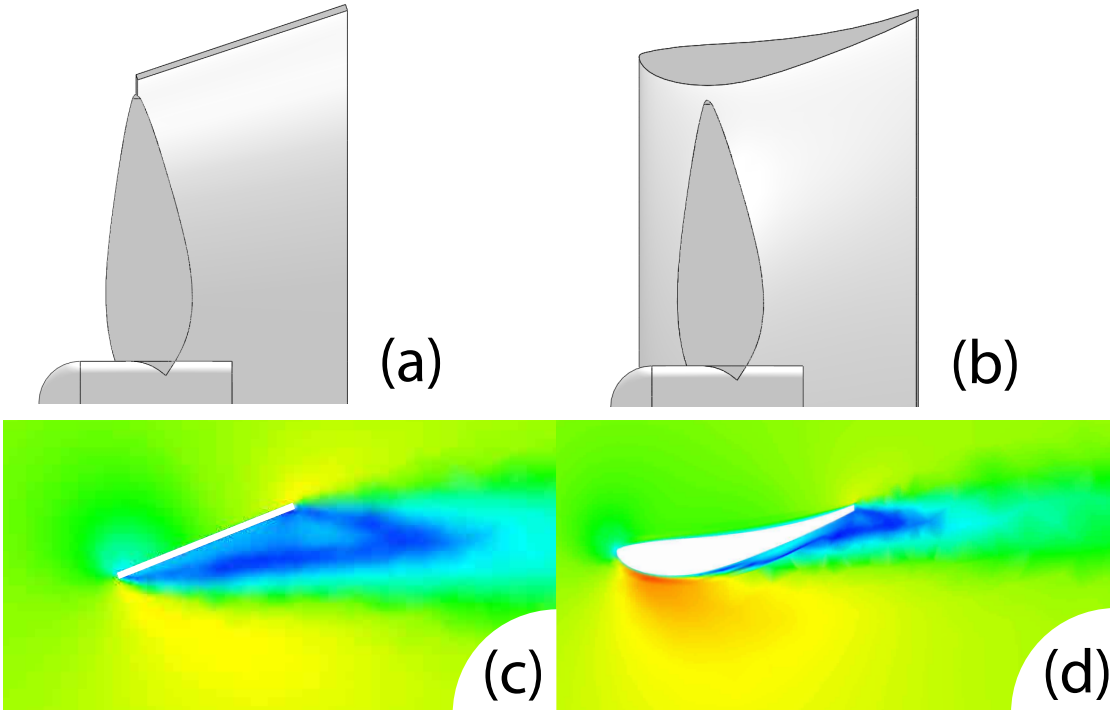

Figure 5.1 – Characteristics of conical and airfoil-shaped diffusers in cross-section views. Conical diffuser in (a) and airfoil-shaped diffuser in (b). Illustration of conical and airfoil-shaped diffuser velocity distributions in (c) and (d).

5.3.1 Influence of the airfoil shape on the power coefficient

Fletcher [47], in 1981, performed wind tunnel experiments to compare the effects of three different high-lift airfoil profiles: NACA 4418 and two LIEBECK variations, L1003 and LA2566. No increase in the maximum C_p was found, although the NACA 4418 airfoil presented a smoother C_p curve with a wider operation interval. Aranake et al. [9, 11], from 2013 to 2015, compared the following airfoils: E423, S1223, NACA 0006 and FX 74-CL5-140MOD. The S1223 high lift airfoil attained a significant amplification of mass flow, proportional to the increase in radial-lift force, evidencing the usefulness of diffusers at low flow speeds.

5.3.2 Influence of the airfoil shape on the pressure distribution

Civalier et al. [30], in 2011, tested the effects of different airfoils on a floating, lighter than air, diffuser-augmented turbine. They tested four different variations of the NACA profile. The study concluded with two main shapes for different purposes: one for generating a higher lift and the other for a higher power coefficient. Venters et al. [150], in 2013, compared the following airfoils: CH 10-48-13 CLmax, E423 and FX 74-CL5-140MOD. They opted for the E423, which resulted in the highest lift coefficient.

5.3.3 Influence of the airfoil shape on the axial velocity distribution

Mehmood et al. [99, 98], in 2012, studied the NACA 0016 and NACA 0018 at different lengths and expansion angles. They reported the velocity distribution obtained for each setup, together with optimal lengths and angles.

5.3.4 Optimization of the airfoil profile

Coiro et al. [32, 35, 36], from 2013 to 2016, conducted a numerical airfoil shape optimization. They obtained a 6.1% increase in the C_p over the turbine using the original diffuser shape. Another optimization was proposed by Song et al. [138], in 2019, working on the DT0814 hydrofoil. They evaluated how the profile's thickness affected the C_p and found varied increases or decreases depending on the associated expansion angle.

Leloudas et al. [88], in 2020, developed a modular optimization for a diffuser with an aerodynamic shape. The numerical analysis had as fixed parameters the throat diameter and volume of the baseline diffuser design. The optimization resulted in a diffuser named SD1, which produced a mean-velocity speed-up ratio of 1.9, a 23% increase over the baseline diffuser.

5.4 Blade-tip effects

Blade-tip vortices have been of great concern when designing wind turbines. For proper rotor design, it is useful to know the behavior of those vortices in the presence of a diffuser encasing the turbine; also how the blade-tip gap affects the C_p^d.

Takashi et al. [142], in 2012, used three-dimensional large-eddy simulations with moving boundary techniques. They observed that the blade-tip vortices induce counter-rotating vortices on the diffuser's inner surface, which helps to weaken them. For compact diffusers, with a length of approximately 0.2 D_r, the blade-tip vortices produced were stronger than those of the bare wind turbine. That occurred due to accelerated inflow, especially near the inner surface of the diffuser. The same was qualitatively evidenced on experimental tests [2].

Saleem and Kim [129], in 2019, performed three-dimensional numerical analysis at multiple flow speeds for tip gaps ranging from 1 to 5% of the diffuser's throat radius. They observed a decrease in the C_p^d at higher tip gaps for flow speeds ranging from 10 to 20 m/s. For 25 m/s flow speeds, an 2.5% increment in C_p^d was observed as the tip gap increased from 1 to 3%.

Lipian et al. [91], in 2020, analyzed velocity fields on the rotor plane, and how the diffuser modifies blade-tip losses. They developed a tip loss correction, using empirical parameters, for models based on the blade element theory. This correction modifies the circulation distribution in the wake by adjusting the rotor solidity.

5.5 Building-augmented wind turbines

Horizontal-axis wind turbines are often employed in urban environments surrounded by buildings that generate similar effects to a diffuser encasing, increasing the turbine's power coefficient. Figure 5.2 illustrates two cases of building-augmented wind turbines.

Figure 5.2 – Illustration of building-augmented horizontal-axis turbines. Bahrain Towers on (a) and The Strata on (b).

Mertens [100], in 2002, went through several wind turbine designs and their feasibility to be installed around buildings. He reminded of the concern about noise emissions those turbines created and addressed the turbine's positioning, which should be ideally on top or sides of the building.

Watson et al. [158], in 2007, performed a numerical analysis of a turbine inside a long diffuser and compared with one-dimensional theory predictions, showing agreement of both. They furthered their work with a numerical analysis of the same setup mounted on a rooftop, which could not be replicated by the same analytical theory. Heo et al. [60], in 2016, performed a numerical analysis on a 110 kW turbine between two buildings. The tests considered varying wind speeds and inflow angles. The buildings presented the same increase in inflow that is observed on a conventional diffuser-augmented turbine. Higher aerodynamic power was reported for inflow angles between -30° and 20° for the building-augmented turbine, when compared to its bare counterpart. For more extreme inflow angles, the performance of the building-augmented turbine sharply decreased. The methodology employed on both of those works might be useful for those with similar goals.

Grant et al. [55, 1], in 2004 and 2008, developed a mathematical model to study the performance of turbines inside a duct to be installed on rooftops. The concept

presented directional sensitivity. They evaluated the energy output of two ducted turbines and compared them with the one from a bare turbine. The data was gathered over a year, accounting for seasonal variation. The bare turbine's annual total was 156 kWh while the two ducted modules generated 147 and 219 kWh.

Petkovic et al. [118], in 2014, performed a numerical analysis using an adaptive neuro-fuzzy method. They designed two buildings with a wind turbine between them and reported the effects of the building's shape on the turbine's power coefficient.

5.6 Curved diffuser

On most diffuser designs, there is no need to prioritize lift generation. Due to that, an airfoil-shaped diffuser can be simplified into a curved thin shape, as from Figure 5.3(a) to 5.3(b). Those curved diffusers (or sometimes called lens/optical diffusers) are often easier to manufacture and attain similar results.

The recirculation zone, detailed in Figure 5.3(d), makes the curved diffuser hydrodynamic-similar to an airfoil. However, that is not always the case, as depending on the curve shape, the recirculation zone may be inexistent. Nonetheless, the upper surface of the curve does not disrupt the flow in an unwanted manner.

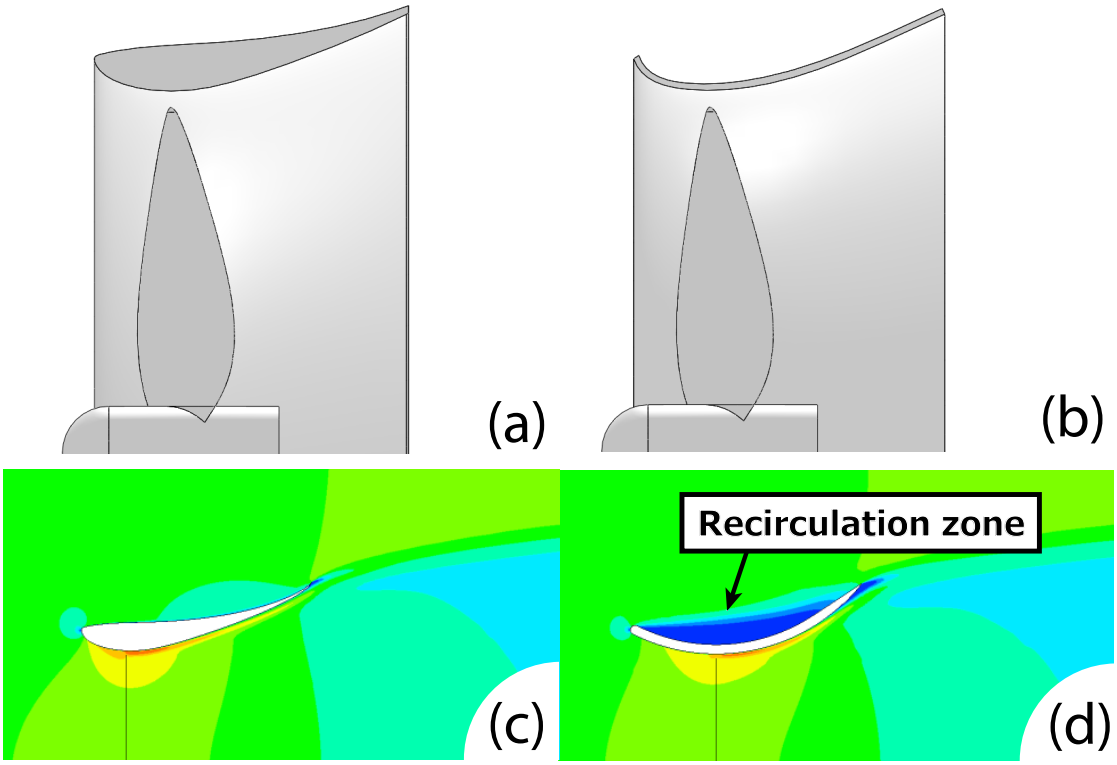

Figure 5.3 – Characteristics of curved diffuser in cross-section views. Airfoil-shaped diffuser in (a) and curved diffuser in (b). Illustration of airfoil-shaped and curved diffuser velocity profiles in (c) and (d), with detail to the recirculation zone that makes the curve shape hydrodynamic-similar to an airfoil profile; reused and edited with permission [41].

Ohya and Karasudani [105], in 2010, analyzed four different curved diffuser configurations. The configuration *C* achieved better results over the others, presenting a C_p^d of 0.54. All tests were experimental, and the proposed *Cii* configuration was chosen to be manufactured and tested on a wind farm.

Nasution and Purwanto [103], in 2011, used numerical tools to compare diffusers with a conical, curved, and an optimized shape. The cross-sections were shaped following the upper surface of the NACA 5807 airfoil. They analyzed the local velocity curves along the diffuser's axis, showing an increase of 65% in the axial velocity of the optimized shape over the conical one. It is essential to remember, when reading the article, that those values are overrated since the curve induces a reduction in the diffuser throat area.

Foote and Agarwal [48], in 2012, proposed a method of curve optimization based on the position displacement of several control points. They analyzed 13 different shapes of different sizes and lengths. On the same line, Amer et al. [6], in 2013, proposed a set of parameters to be changed to create a range of diffuser shapes to be tested. Results revealed that values of D_d/D_r between 1.5 and 2 produced the highest increases in axial velocity. They also evaluated that convex diffuser shapes are more efficient than conical or concave ones. In both analyses [48, 6], only numerical tools were used.

5.7 Diffuser length

To increase the diffuser-augmented turbine's performance, it is common to search for ways to increase the A_d/A_r ratio.

The most direct method to do that is by increasing the diffuser's expansion length, L_e. This method does not generate an impact on the expansion angle, thus lessening the possibility of flow separation.

Multiple authors performed numerical analyses to evaluate the effects of the diffuser's length. While maintaining the same expansion angle and inlet diameter, they observed how the diffuser's length influenced the flow's maximum axial velocity, u_{max}, in a standalone diffuser. Matsushima et al. [97] and Ohya et al. [109], both in 2006, observed a 30% increase on u_{max} when increasing the L_e/D_i ratio from 0.5 to 2; increasing the length further produced only marginal results.

In the same manner, Buehrle et al. [22], in 2013, and Shi et al. [135], in 2015, performed tests on diffuser-augmented turbines. Buehrle et al. [22] verified a 10% increase on u_{max} when increasing the L_e/D_i ratio from 0.25 to 0.75. Shi et al. [135] verified increases lower than 10% on u_{max}, but not properly specified by the authors; those changes were evaluated for the $0.5-2.0$ L_e/D_i ratio interval.

On a diffuser-augmented turbine with a curved diffuser, Ohya and Karasudani [105], in 2010, observed a $20-25\%$ increase in the C_p for an increase in L/D_r from 0.1 to 0.2; those gains stabilized for lengths above $0.2D_r$.

5.8 Flanges

Flanges (or sometimes called brims), as illustrated by Figure 5.4(a), disrupt the flow above the diffuser, increasing the turbulence in its wake. It creates recirculation zones, illustrated by Figures 5.4(b) and 5.4(c), that promote a decrease of pressure behind the diffuser, thus increasing the mass flow through the inlet.

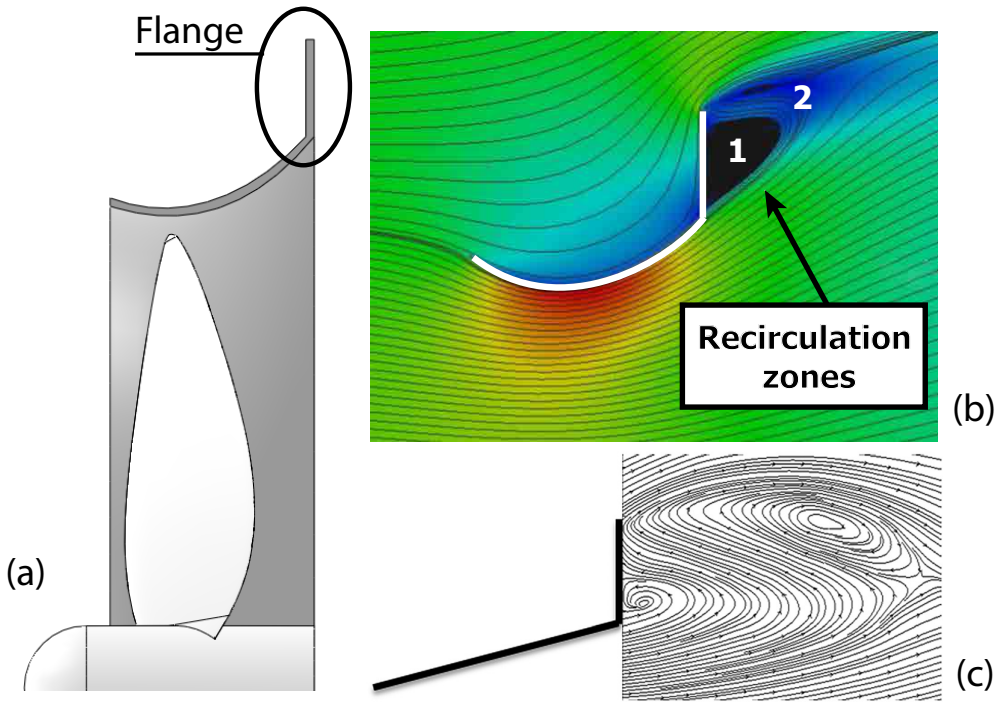

Figure 5.4 – Illustration of flange aspects in cross-section views. Detail to flange on curved diffuser in (a). Illustration of velocity field and recirculation zones from axisymmetric numerical analysis in (b), reused and edited with permission [78]. Particle-image velocimetry of recirculation zones in (c), reused with permission [25].

The flange's usefulness, and the influence of its length on the C_p^d, has been a topic studied in experimental works by several authors [105, 82, 61]. They all reported increases in the power coefficient at varying degrees. Numerical analyses have been performed to observe the effect of the flange's height in more detail [4, 38, 67, 97]. The power coefficient increased for flange height intervals between $0 - 0.15D_r$, whereafter, it only decreased or increased marginally.

Setoguchi et al. [131], in 2004, studied the static pressure distributions inside the diffuser in different configurations for varying flange's heights. Lipian et al. [92], in 2015, performed a study in the same vein but observing axial velocity profiles.

Olasek et al. [115], and Kulak et al. [84], in 2016, used PIV techniques to observe the flow inside three diffusers with flanges that had the same geometry but differed in size. The obtained velocity distribution in the radial direction was compared with numerical analysis results and pneumatic measurements.

Kardous et al. [73, 72] and Chaker et al. [25], in 2013 and 2016, observed two counter-rotating vortices at the diffuser's wake, created due to the presence of a flange. This phenomenon is illustrated on Figure 5.4(c). They observed how those vortices changed according to the flange height. Toshimitsu et al. [145], in 2008, observed two vortices at their flanged diffuser-augmented turbine's wake. They reported that one vortex near the flange acts to increase the inlet flow while another vortex further downstream acts as a blockage.

Another topic that has been receiving recent attention is the flange's inclination. Heikal et al. [59], in 2018, achieved a C_p^d of 0.57 at a flange inclination angle of 10 degrees, about 28% higher when compared to the C_p^d of the diffuser-augmented turbine with a vertical flange. Kale et al. [70], in 2013, reported the changes in the diffuser's exit pressure due to a flange inclination of 10 degrees. El-Zahaby et al. [44], in 2017, evaluated the maximum axial velocity for flange inclination angles ranging from -25 to 25 degrees.

One other innovation, in 2015, was Hu and Wang's [63] self-adaptive flanges, which promoted a controlled re-energization of the flow inside the diffuser. No improvements in the C_p^d were observed when compared to a rigid flange. However, self-adaptive flanges reduced the wind load acting on the diffuser by 34.5%.

5.9 Flow mixers

Flow mixers are classified as features applied to the diffuser to modify the flow in the diffuser-augmented turbine's wake. Arguably flanges would also be considered flow mixers. However, due to the research interest on flanges, a separate section was

dedicated to them.

5.9.1 Control plates

Figure 5.5 – Illustration of control plates on diffuser, reused with permission [108].

Ohya [108], in 2014, proposed the use of control plates, Figure 5.5, coupled to the body of the diffuser to create a more structured vortex flow. Based on a study on rectangular bodies, it was evidenced that the flow between those controlled plates created a stronger vortex shedding. In opposition to the usual practices on aerodynamic machinery, this effect is desirable to diffuser-augmented turbines. The low-pressure region it creates behind the turbine increases the mass flow that passes through the rotor. The effects of a different number of control plates and their influence in the power coefficient were analyzed. The configuration with six control plates achieved the highest increase in the C_p^d.

Watanabe et al. [157], in 2019, tested using numerical analysis and experiments several configurations of more practical control plates. They verified the same results as Ohya. The configuration with six control plates achieved a maximum increase in the C_p^d of 3.8% over the configuration without control plates.

5.9.2 Lobed diffusers

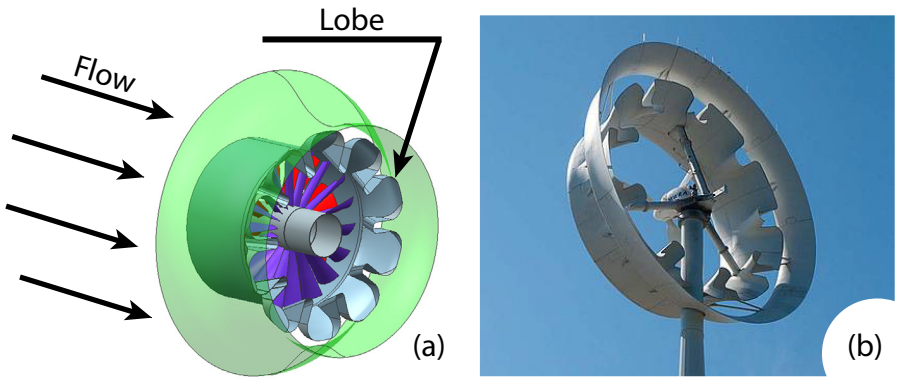

Figure 5.6 – Lobed diffusers viewed from the back. Scheme in (a), reused and edited with permission [57]. Lobed diffuser by FloDesign, in (b), courtesy of Ewan O'Sullivan [123].

Lobed diffusers, or lobed ejectors, as illustrated in Figure 5.6, apply the technology of lobe forced mixers, commonly seen on nozzle turbofans engines, to diffuser-augmented turbines. The lobes create counter-rotating vortices, which are then expanded inside the diffuser. This effect promotes a lower pressure gradient behind the diffuser and delays the boundary layer separation. Han et al. [57], in 2015, studied the effect of this type of diffuser, focusing on the vortices' structures that were created due to it. The maximum vorticity lowered about 75% in the axial region of $0-0.5D_r$, decreasing slowly after.

5.9.3 Vortex generators

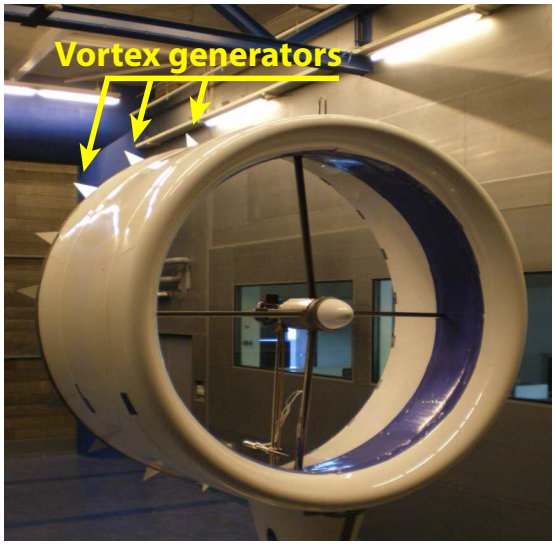

Figure 5.7 – Illustration of vortex generators on diffuser-augmented turbine [144].

Vortex generators, as illustrated in Figure 5.7, are triangular additions to the diffuser that possess the same purpose as gurney flaps when used on diffuser-augmented turbines. However, the area occupied and size are smaller, facilitating the manufacture, installation, and reducing the diffuser projected area.

Ten Hoopen [144], in 2009, performed an experimental and numerical study on vortex generators for diffuser-augmented turbines. They observed a maximum increase of 9% on the C_p^d due to the addition of 37 vortex generators to the diffuser. The author also compared the vortex generators with flanges. In comparison with their projected areas, the vortex generators outperformed flanges by 10% in the C_p^d increase.

5.10 Frontal nozzles

Frontal nozzles, as illustrated in Figure 5.8, are an expansion on the inlet opening of the diffuser, that act as a concentrator of the mass flow. Even though most of the diffuser designs include nozzles to a certain extent, few works studied the effects of the nozzle with a clear comparison of the same design with and without this feature.

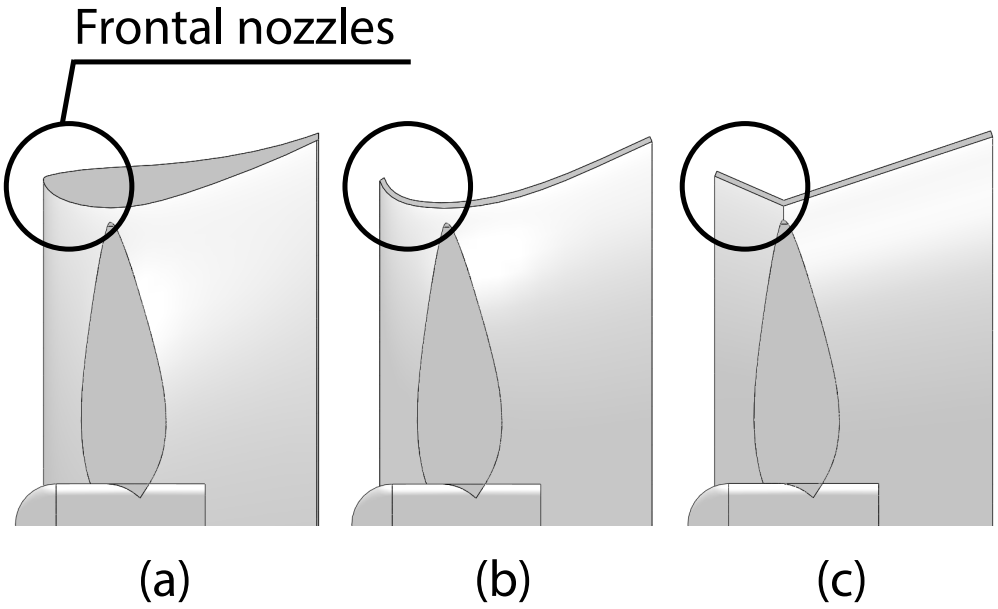

Figure 5.8 – Detail to frontal nozzles in cross-section view of diffuser-augmented turbines. Frontal nozzles in: airfoil-shaped diffuser in (a), curved diffuser in (b), conical diffuser in (c).

Kosasih and Tondelli [82], in 2012, tested diffuser-augmented turbines with and without nozzles. Results showed negligible improvements due to the nozzle addition. However, the nozzles' employment allowed the diffuser-augmented turbine to operate at higher yaw angles without considerable decreases in the C_p.

Anzai et al. [7], in 2004, and Amer et al. [6], in 2013, focused their study on the effects of the geometry of the nozzle. Anzai et al. [7] performed experimental tests to study how different ratios of nozzle diameter affected the power coefficient. Amer et al. [6] conducted a numerical analysis and studied how different shapes of nozzles influenced the axial velocity profile inside of it.

5.11 Multi-slots

Multi-slots diffusers, as seen in Figure 5.9, are designed with the purpose of re-energizing the expanded flow inside the diffuser, enabling higher expansions while preventing the flow separation from the diffuser's inner surface.

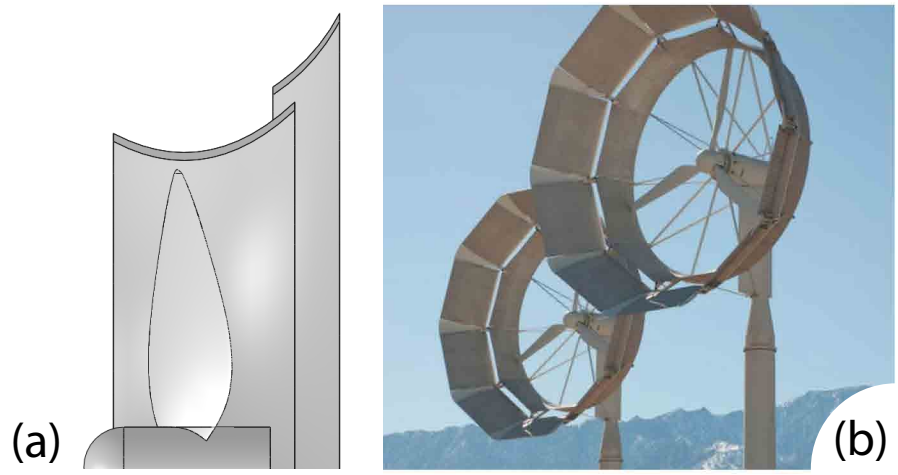

Figure 5.9 – Multi-slots diffusers. Cross-section view in (a). Commercial design by FloDesign, in (b) [71, 56].

Several authors tested multi-slots diffusers and reported their results in terms of axial velocity, pressure distribution, and power coefficient [65, 94, 119, 121, 128, 140]. Oman et al. [116], in 1977, carried out detailed experiments studying the influence of different parameters of a multi-slots diffuser-augmented turbine, such as the expansion angle and each slot's radial distance from the axis.

Dighe et al. [39], in 2019, performed a numerical analysis to evaluate the effects of the radial gap length, the space between the secondary slot and the diffuser, and the slot's angle. They reported increased thrust on the diffuser-augmented turbine at higher radial gap lengths and decreased thrust at higher slot angles. Koç and Yavuz [80], in 2019, performed a numerical analysis to optimize the secondary slot based on measurements of the flow's maximum axial velocity. The parameters included in the study were the secondary slot's length, angle, and distance to the diffuser exit. They observed an increase in u_{max} of 9% over the diffuser without a secondary slot. Those results were obtained for a secondary slot with a length of 40% of the diffuser's chord length.

Keramat Siavash et al. [75], in 2020, developed a multi-slots modular diffuser that could be compartmentalized in different configurations. They verified not only changes in the power coefficient but also some configurations that allowed the diffuser-augmented turbine to operate at a wider TSR range.

A gap in knowledge remains when discussing multi-slots diffuser-augmented turbines. A comparison between a multi-slots diffuser and a conventional one, of similar shape, at the same A_d/A_r ratio, is worthy, along with a study comparing their respective C_p^d for varying A_d/A_r ratios, to investigate the re-energizing effect.

5.12 Multi-turbine system

Instead of changing further their diffuser designs, some authors opt for studying the effects of the arrangement of multiple turbines, and how each diffuser-augmented turbine influenced the other. Figure 5.10 illustrates an arrangement of five diffuser-augmented turbines, with detail to the system gap parameter, s. The objective is to attain a mean power coefficient higher than the one of standalone turbines.

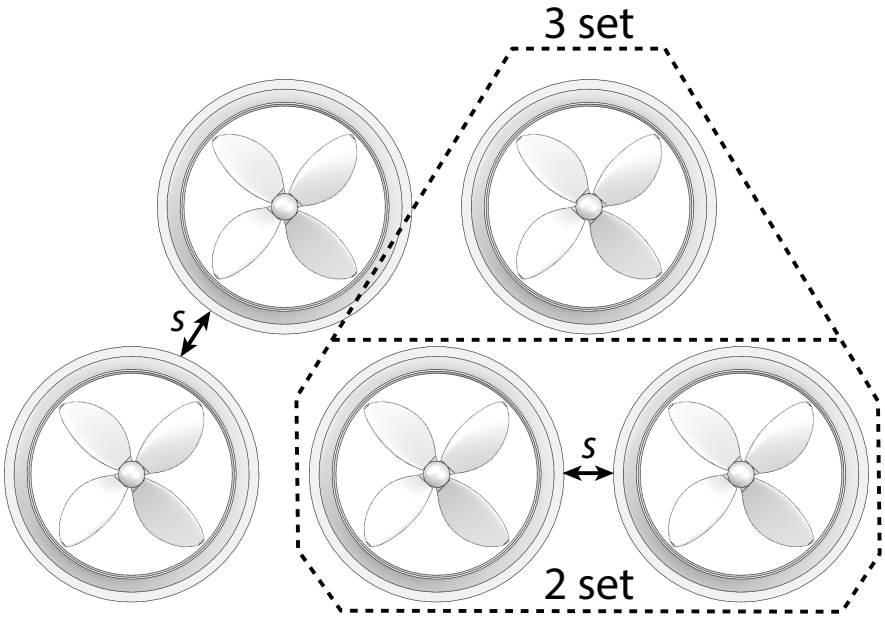

Figure 5.10 – Illustration of five diffuser-augmented turbine's arrangement, with detail to Multi-turbine system's gap parameter. Distinction of two and three turbine's arrangement.

Most studies seek the optimum distance between two diffuser-augmented turbines, which generates the maximum mean C_p. The following results compare the mean C_p of

the diffuser-augmented turbine arrangement with the C_p of a single diffuser-augmented turbine of the same type. Results for a system of two diffuser-augmented turbines showed an improvement of 8% in the C_p [110], for a gap ratio, s/D_d, of 0.20; different gap ratios attained lower improvements. In systems of three diffuser-augmented turbines, improvements ranging from 9% to 12% in the C_p were reported for gap ratios of 0.20 [54, 110, 156]. Five diffuser-augmented turbines' systems showed an improvement of 21% in the C_p at gap ratios of 0.20 [155, 161].

Research opportunity exists for turbine arrangements in the same horizontal plane, following configurations similar to Figure 5.11. Such configurations are already studied on bare wind turbines [29, 86]: on the influence of the wake flow on the turbines downstream, especially concerning wind farms setups.

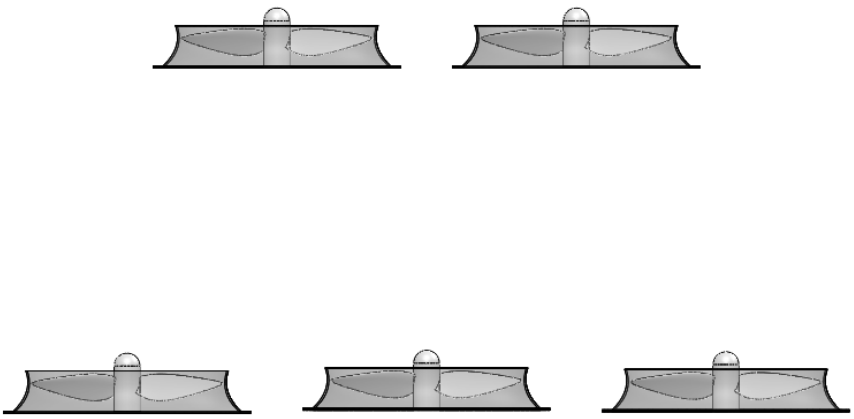

Figure 5.11 – Alternative turbine arrangement proposed for research.

5.13 Simultaneous diffuser-rotor design

It is common to change the rotor's shape to increase the bare turbine's power coefficient. When designing a diffuser, most works do not change their already existing rotor project and try to adapt the diffuser to it. This process is not optimal, as the rotor was not planned to operate with a diffuser enhancing it.

Van Dorst [147], in 2011, performed an optimization for the rotor blades considering an already defined diffuser design. They defined the optimal rotor loading through

a one-dimensional analysis and used that as a basis for the strength of a vortex cylinder in the actuator disk model. The model resulted in the velocity distribution for the optimal loading factor, which was used to design a new rotor though the blade element momentum method. Experimental tests on the new rotor showed an improvement of 15% in the C_p^d over the previous rotor employed on the same diffuser.

Oka et al. [111, 112, 113], from 2013 to 2015, and Khamlaj et al. [77, 76, 78], in 2017 and 2018, applied numerical algorithms to design both the diffuser and rotor simultaneously, considering that they would be operating as a diffuser-augmented turbine. The algorithms employed were based on multi-objective genetic methods. The method process the variation of several parameters regarding the diffuser's or the blades' shape, testing thousands of design points for diffuser-augmented turbines. Pareto optimal solutions [162] were applied to define the best geometries for further study. The chosen geometries were the ones that maximized C_p^d and minimized size. Oka et al. [113] also validated their numerical analysis through experiments and obtained a C_p^d of 0.62.

5.14 Twin-rotors on diffusers

The addition of a diffuser to a turbine increases the rotor's axial load as a side effect of increasing the power coefficient. Wang et al. [154], in 2015, observed increases ranging from 2.0 to 3.5 on the maximum tensile strain of the blade roots, when comparing the situation with and without a diffuser.

Twin rotors, as illustrated by Figure 5.12, are proposed to distribute the increased turbine load and increase the turbine's power coefficient by making use of the remaining kinetic energy in the wake. They are a set of two counter-rotating rotors on the same turbine axis.

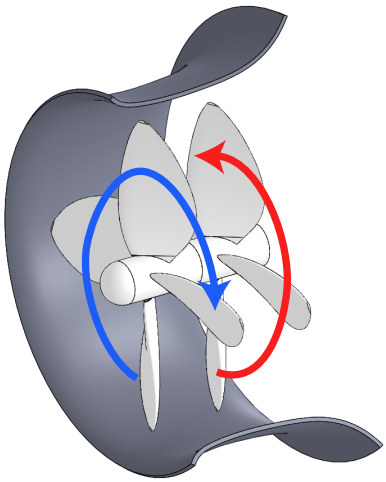

Figure 5.12 – Illustration of diffuser-augmented twin-rotor turbine, and its counter-rotating aspect.

Lipian et al. [90, 91], in 2019 and 2020, tested a set of twin-rotors with a conical diffuser. They compared the results of a bare turbine, diffuser-augmented turbine, twin-rotor bare turbine, and diffuser-augmented twin-rotor turbine. The diffuser-augmented turbine presented a 28% increase in the maximum C_p^d over its bare turbine counterpart. The addition of twin-rotors provided no changes on C_p^d, but it reduced the thrust coefficient from the upstream rotor, distributing the load more evenly.

Kumar et al. [85], in 2019, established a theoretical model to evaluate the power output of diffuser-augmented twin-rotor turbines. The results depend on a parameter governed by the area-weighted sum of the loading coefficients of both rotors. The model considers diffuser geometry, back pressure, and flow-efficiency parameters.

5.15 Yaw and shear flow effects

Horizontal-axis turbines, and, as a consequence, diffuser-augmented turbines, present a reduction in their C_p when under effects of yaw or shear. Those motions quicken the boundary layer separation at the rotor and at one of the diffuser's surfaces, raising new concerns in diffuser-augmented turbines. However, Kosasih and Tondelli [82], in 2012, verified that at low yaw angles, 5 degrees, this misalignment in the flow might be

mitigated by the employment of nozzles.

Igra [66, 64, 65], from 1977 to 1981, reported the effects of a range of yaw angles, from 0 to 30 degrees, on a diffuser-augmented turbine. He evaluated how the yaw angle affected the drag, lift, diffuser's outlet pressure, and diffuser's performance. The results were compiled for eight different diffuser models. The *Cii*, and *Ci* models attained a higher C_p at higher yaw angles, 30 degrees, than at lower ones.

On the topic of hydrokinetic turbines, Scherillo et al. [130], in 2011; Shahsavarifard and Bibeau [133, 132, 134], in 2015 and 2020; and Coiro et al. [31], in 2017, tested several diffuser-augmented turbine's designs at yawing conditions in towing tanks and circulating water channels. They reported variations in the C_p smaller than 5% up to yaw angles of 10 degrees.

Ke et al. [74], in 2020, performed a numerical analysis to study a diffuser-augmented turbine under different yaw and shear flow effects. Under higher shear flow conditions, they reported more severe fluctuations on the turbine's load, which were only amplified by the diffuser; a more significant concern for fatigue design on diffuser-augmented turbines under those conditions is necessary. Yawed conditions reduced the diffuser-augmented turbines optimum operation point to lower tip-speed-ratios, also reducing its C_p.

5.16 Other diffuser concepts

Beyond those mentioned here, other less studied diffuser's geometries exist, such as the vorticity based diffuser, aiming to reduce the wake pressure and prevent flow separation [95, 114]; the mixer-ejector diffuser, which uses a pump and a ring of rotating blades to mix the low energy flow that exits the turbine with the high energy flow the enters through a secondary slot [122]; the dynamic diffusers, which rotates along with the rotor on its axis [160]; lighter-than-air diffusers made for floating with lightweight materials [151, 152, 159]; and the vortex enhancer diffuser, which creates a rotating flow on the diffusers' wake [14]. The reader may gather more information on different diffuser designs through the work of Agha et al. [5], where they introduce and discuss several different patented diffuser technologies.

6 Metrics of assessment

The current chapter complements Chapter 4 in the presentation of parameters related to diffuser-augmented turbines. The objective is to propose metrics that will enable a unified evaluation of several diffuser-augmented turbines.

As many authors try to progress in favor of the diffuser technology applied to horizontal-axis turbines, an overflow of outstanding performance enhancement reports has appeared in the literature on the last years. Despite the results shown, it is still unclear whether the addition of a diffuser is preferred instead of increasing the rotor's diameter. Several factors would have to be evaluated to assess this problem, such as size, material, and manufacturing limitations. Also, all those factors need to be evaluated for each specific case.

To try to shed some light on this discussion, a performance assessment of several diffusers reported in the literature will be presented. The performance assessment will follow the metrics proposed in the present chapter, divided into power coefficient and tip-speed-ratio metrics. Those metrics are rather conservative ones, downgrading the diffusers' enhancement but showcasing its actual potential nonetheless.

6.1 Power coefficient metrics

The most common metric used by authors to report their diffusers' performance is the maximum C_p for a given interval of tip-speed-ratios; parameters defined on Equations (4.3) and (4.5) respectively. Those are the two main parameters to define the turbine's working conditions. However, this metric compares the power generated by the diffuser-augmented turbine to the power available to the rotor, even though the power available to the diffuser-augmented turbine is higher than the one available to the rotor.

To consider the diffuser's size and make a fairer assumption of the diffuser's worth, the comparison should be made between the generated power and the power available to the turbine. This comparison was defined as the diffuser-augmented turbine's actual power coefficient, C_p^d, on Equation (4.4), which takes into consideration the

diffuser's maximum cross-sectional area;

$$C_p^d = \frac{P_{diffuser}}{\frac{1}{2}\rho U^3 A_d}. \tag{4.4}$$

To go one step further, a comparison is made between the C_p^d and a baseline: the power coefficient of its bare turbine, C_p^b,

$$C_p^b = \frac{P_{bare}}{\frac{1}{2}\rho U^3 A_r}. \tag{4.2}$$

The diffuser-enhancement parameter, E_d, is defined as

$$E_d = \frac{C_p^d}{C_p^b} - 1. \tag{6.1}$$

The diffuser-enhancement parameter intends to provide a measure of the actual hydrodynamic improvement for power conversion associated with the diffuser. To do that, it is assumed that the bare turbine scaled up to the diffuser's diameter of its shrouded version does not alter its maximum power coefficient. Therefore, E_d, as defined by Eq.(6), is the relative difference between the maximum power converted by a diffuser-augmented turbine and the maximum power converted by a bare turbine with the same diameter of the diffuser. In this sense, $E_d = 0$ means that installing the diffuser or simply scaling the rotor up to the diffuser's diameter has the same effect in terms of power production. Conversely, $E_d > 0$ means that simply increasing the area swept by the rotor to match the diffuser area does not elevate the power conversion as the diffuser-enhancing does. In other words, E_d is related to a more effective diffuser enhancing.

As stated, the diffuser-enhancement parameter makes a comparison similar to the one illustrated in Figure 6.1(b), whereas previous power coefficient metrics were more akin to Figure 6.1(a). It evaluates how much the diffuser increased the original bare turbine's potential, no matter whether it was high or low before. It is crucial to notice that E_d is a metric that judges how well designed the diffuser is for its size. If the reader has no concern about the diffuser's size in their design, the metrics E and C_p^d will be of less use to them.

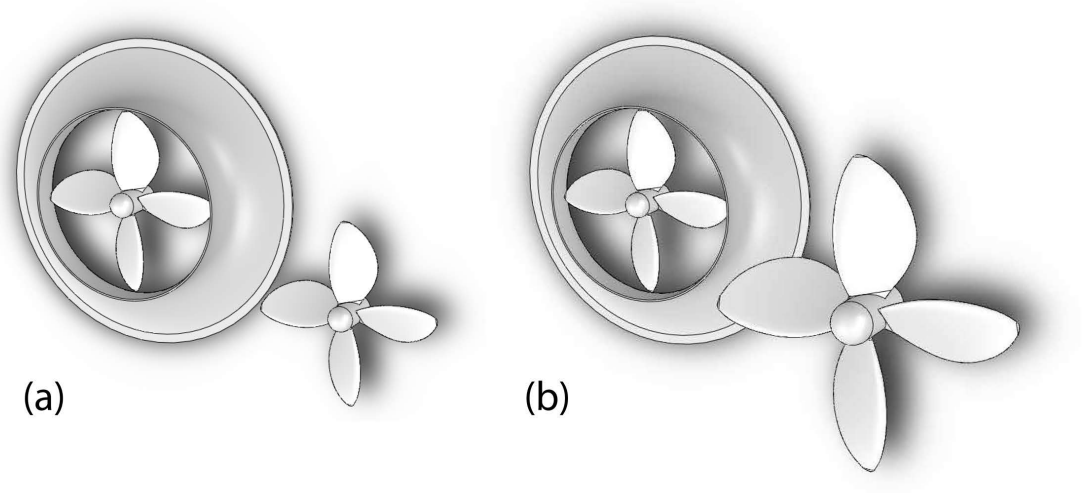

Figure 6.1 – Power coefficient comparison between diffuser-augmented turbine and bare turbine. Comparison on usual C_p metric in (a). Comparison on proposed E_d metric in (b).

6.2 Tip-speed-ratio metrics

In practice, it is usual to seek the optimum TSR interval, i.e., the interval in which the power coefficient is maximum, or close enough to it. The interval width and position may vary for each turbine. As a start, two parameters are defined to characterize the TSR and its variations during situations with or without a diffuser: TSR_{width} and TSR_{center}, as illustrated in figure 6.2.

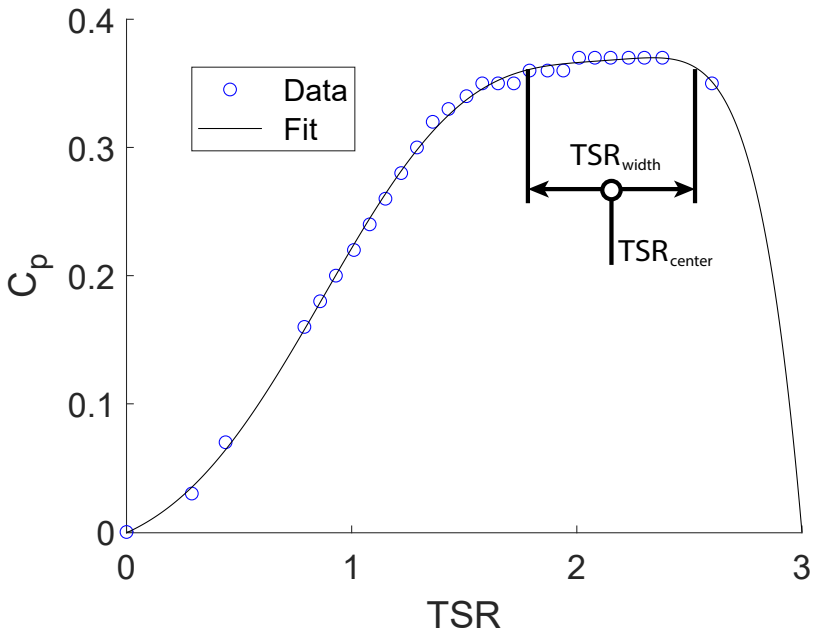

Figure 6.2 – TSR_{width} and TSR_{center} illustration on a power coefficient curve. Data obtained from previous work [104].

The TSR_{width} represents the size of the turbine's optimum operation interval, the TSR interval where the C_p is at its maximum. Turbines with a higher TSR_{width} are desirable by their wider operation interval and smaller fluctuations due to environmental changes.

The TSR_{center} is the optimum operational interval center. It represents the center point of this operational interval. This parameter will help track changes in the operational interval positioning. A turbine with a high TSR_{center} operates at lower open flow speeds if compared to ones with smaller TSR_{center}. If the purpose is, for example, to utilize low-grade wind energy, a turbine with a high TSR_{center} is desirable.

The parameter TSR_{width} is defined by two TSR points, TSR_1 and TSR_2, such that

$$TSR_{width} = TSR_2 - TSR_1 \tag{6.2}$$

and

$$C_p(TSR_1) = max(C_p) - 0.01, \tag{6.3}$$

$$C_p(TSR_2) = max(C_p) - 0.01, \tag{6.4}$$

$$TSR_2 > TSR_1. \tag{6.5}$$

The value 0.01 was chosen as a defining constant to create a standard for TSR_{width} where the associated C_p is always kept close to the maximum. It adequated well to most of the data investigated.

The parameter TSR_{center} is defined as

$$TSR_{center} = \frac{TSR_2 + TSR_1}{2}. \tag{6.6}$$

To evaluate the performance of a diffuser, comparisons are necessary between the tip-speed-ratios of turbines with and without the addition of diffusers.

The TSR^*_{width} is a comparison between the operational interval of the diffuser-augmented turbine and the bare turbine, defined as

$$TSR^*_{width} = TSR^d_{width} - TSR^b_{width}, \tag{6.7}$$

where TSR^d_{width} and TSR^b_{width} represent the diffuser-augmented turbine's and the bare turbine's TSR_{width}, respectively.

The TSR^*_{center} is how much the center of the operational interval changed in position, comparing the diffuser-augmented turbine with its bare counterpart. The TSR^*_{center} is defined as

$$TSR^*_{center} = TSR^d_{center} - TSR^b_{center}, \tag{6.8}$$

where TSR^d_{center} and TSR^b_{center} represent the diffuser-augmented turbine's and the bare turbine's TSR_{center}, respectively.

7 Performance assessment

Data was gathered from the work sample of 155 articles, and the characteristics of 73 diffuser-augmented turbines were registered. Geometric and performance data on each diffuser-augmented turbine was collected. The data is summarized in Appendix B, for performance parameters, and Appendix C, for geometry.

The present chapter analyzes the recorded diffuser-augmented turbines based on the metrics proposed in Chapter 6. The results presented showcase not only details about specific designs but also essential characteristics of diffuser-augmented turbines.

Comparisons are presented between the C_p metric, the C_p^d metric, and how those results translate based on E_d. A more in-depth analysis is performed over tip-speed-ratio, diffuser diameter, diffuser-augmented turbine's power coefficient, and diffuser-enhancement.

7.1 Power coefficient distribution

An analysis based on the power coefficient informs us about the initial idea of a diffuser's value. The power coefficient was evaluated based on the metrics proposed in Equations (4.3), (4.4) and (6.1). The aim is to present to the reader what is to be expected of diffuser-augmented turbines in terms of the power coefficient. This section analyzes a collective of 60 diffuser-augmented turbine designs. Figure 7.1(a) presents the distribution of the maximum C_p achieved, reported by their authors. Figure 7.1(b), on the other hand, presents how those values translate when evaluating in terms of C_p^d, i.e., considering the diffuser maximum cross-sectional area.

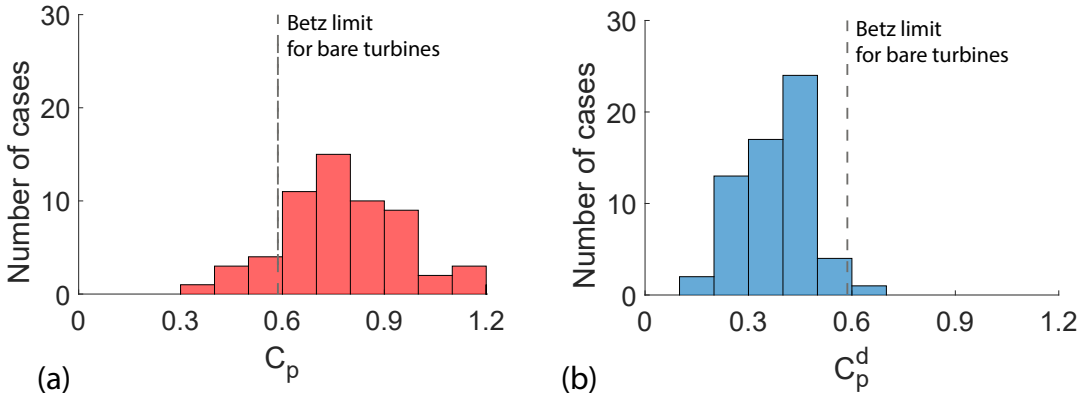

Figure 7.1 – Distribution of diffuser-augmented turbines found on the literature based on power coefficient. (a) Based on C_p metric. (b) Based on C_p^d metric.

A total of 52 diffuser-augmented turbines achieved a C_p higher than the Betz limit for bare turbines; only 8 reported a lower C_p. The reported maximum C_p presented a mean value of 0.75. On the other hand, only one diffuser-augmented turbine achieved a C_p^d higher than the Betz limit for bare turbines; 59 of them reported a lower C_p^d. The achieved maximum C_p^d presented a mean value of 0.37.

That one design beyond the Betz limit for bare turbines is the one by Oka et al. [113], in 2015. It achieved a C_p^d of 0.62. This design will be commented further on Section 7.3. It is important to remember that, as mentioned in Chapter 4, the energy extraction limit for diffuser-augmented turbines is different from the Betz limit established for bare turbines.

A total of 51 diffuser-augmented turbines had enough data to be analyzed in terms of diffuser-enhancement, i.e., the gain that a diffuser-augmented turbine has over a bare turbine of the same size. Figure 7.2 presents the E_d distribution of those designs.

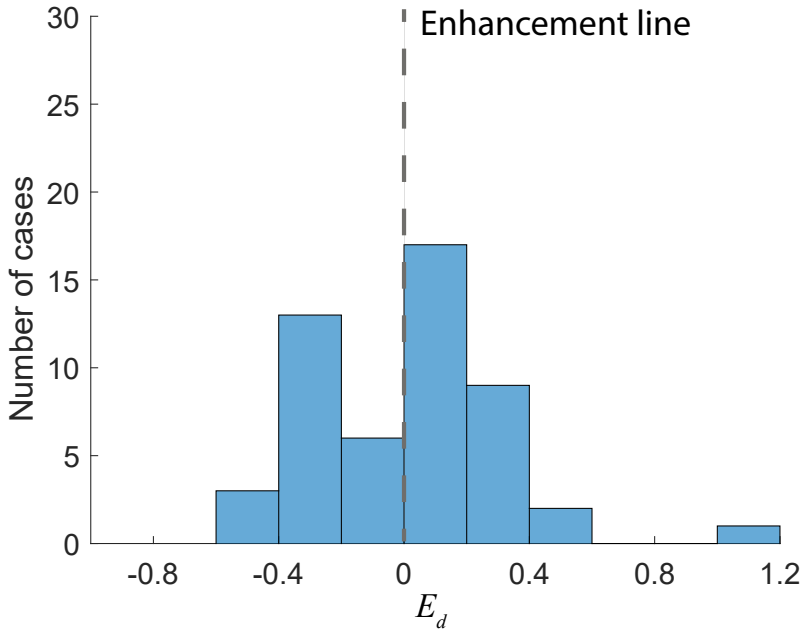

Figure 7.2 – Distribution of diffuser-augmented turbines found on the literature based on E_d.

Results showed that, in 58% of the evaluated cases, the power coefficient of a diffuser-augmented turbine was higher than that of a bare turbine of the same size.

From those 51 designs, 22 presented E_d values lower than 0. In those cases, the alternative of increasing the turbine's diameter might have been a better choice than employing the diffuser. However, 29 designs presented E_d values higher than 0. For those, the diffuser not only increased the turbine's power coefficient, but it was also the better option to increase its power for the given area.

The sole design that presented a E_d of 1.04 was the one by Kosasih and Saleh [83], in 2016; this design will be commented further on Section 7.4. In comparison, the design by Oka et al. [113], commented previously in Figure 7.1(b), does not achieve such distinction when analyzed based on E_d. That is because E_d evaluates the increase in C_p^d in comparison to the original bare turbine's C_p^b. In the case of the design proposed by Oka et al. [113], the original bare turbine already had a high power coefficient; even though it achieved the highest C_p^d, the diffuser-enhancement was not as pronounced.

7.2 Diffuser influence on tip-speed-ratio

Along with the power coefficient, the tip-speed-ratio defines the turbine's operation. How the diffuser influences this parameter is an important analysis that the present section discusses. To achieve that, the metrics proposed on Section 6.2 are employed to evaluate changes to the optimum TSR interval.

The dispersion of the TSR^*_{width} and TSR^*_{center} for 34 diffuser-augmented turbines is presented on Figure 7.3. Each of those points refers to a turbine, comparing the situation with and without the diffuser.

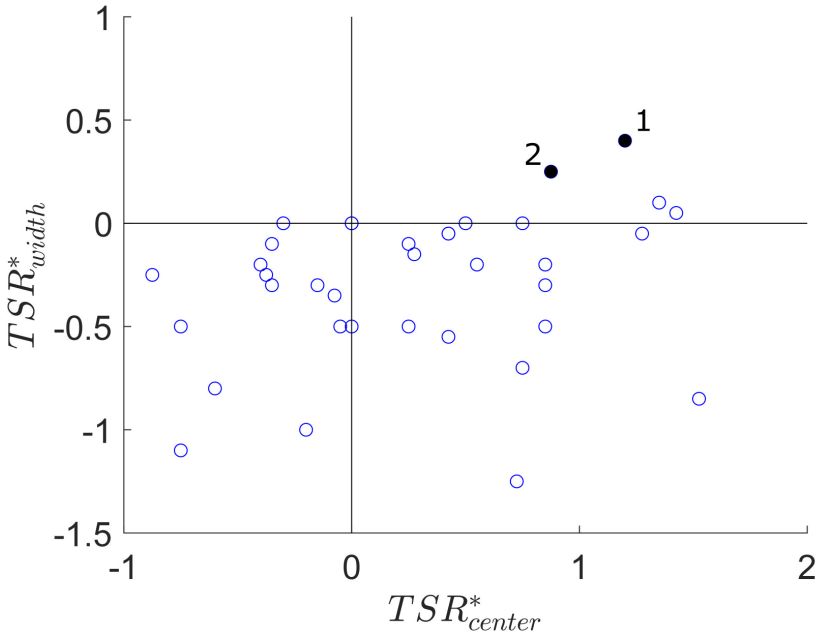

Figure 7.3 – Influence of diffuser on TSR. Comparison of changes between bare turbine and diffuser-augmented turbine. Two design points of interest are highlighted.

Figure 7.3 is divided in quadrants. The top ones, populated by 4 turbines, represent those turbines that developed a plateau in their power coefficient curve after being coupled with a diffuser; they gained a wider operational range. The bottom quadrants, with 26 turbines, represent those that developed sharper power coefficient curves; their operational range became smaller. To the right, 19 turbines now operate at higher rotation.

To the left, after being enhanced with diffusers, 13 turbines now operate at lower rotation.

It is noticeable that the use of diffuser-enhancing technology modified the turbines towards a smaller operational range. However, it also provided flexibility on the range of the operational speed. Based on the diffuser design employed, it is possible to push diffuser-augmented turbines to operate at lower or higher flow speeds. The turbines at the top-right quadrant possess two desirable characteristics: a wider operational range and the possibility to work at lower flow speeds.

The first design point highlighted in Figure 7.3, represents a diffuser-augmented turbine designed by Riglin et al. [126], in 2014. They worked with hydrokinetic turbines and proposed an optimization on conical diffusers with flange, reporting the results of their numerical analysis. The maximum C_p^b achieved for the bare turbine was at the TSR interval of $1.20 - 2.00$. The diffuser-augmented turbine achieved its maximum C_p^d at the TSR interval of $2.20 - 3.40$. The TSR^*_{width} obtained was of 0.4 and the TSR_{center} shifted from 1.60 to 2.80. The C_p^d achieved was 0.22, lower than the average observed in Section 7.1. Concerning the experiments, data points reported were few, and no similar results, with regards to TSR, were found in other works by the same authors [125, 127], even though new proposed designs by the authors achieved higher C_p^d values.

The second highlighted design point was proposed by Tampier et al. [143], in 2017. They performed a numerical analysis over an airfoil-shaped diffuser coupled to the hydrokinetic turbine. Results for the bare turbine presented an TSR optimum interval of $3.50 - 4.25$. The diffuser-augmented turbine optimum TSR interval was $4.25 - 5.25$. The TSR^*_{width} achieved was of 0.25 and the TSR_{center} shifted from 3.92 to 4.75. The C_p^d achieved was of 0.19, lower than the average observed in Section 7.1.

Both design points reported high C_p values. However, since the size of their designs was much larger than the rotor, the attained C_p^d was lower than the average C_p^d of 0.37, reported on Section 7.1. No correlation was found between C_p^d and the corresponding TSR^*_{center}.

7.3 Well designed diffuser-augmented turbines

A diffuser expands the flow inside it, increasing the mass flow in the inlet. That expansion correlates to the difference in area between the inlet and the outlet. Studying the effects of the expansion can help identify good diffusers' designs, even though E_d has no regard for this area ratio.

In the following analysis, the area ratio is described as A_d/A_r, where, as mentioned in Chapter 4, A_d is the diffuser's maximum cross-sectional area, and A_r is the rotor spanning area.

To point the traits of the highest achieving designs, Figure 7.4 shows a dispersion of 52 diffuser-augmented turbines by their C_p^d and A_d/A_r.

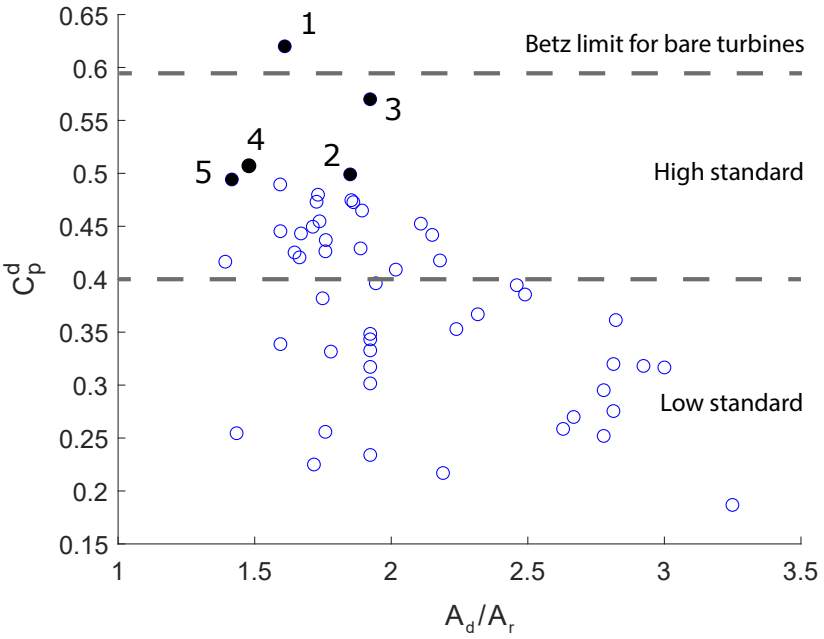

Figure 7.4 – Dispersion of the diffuser-augmented turbines respective to C_p^d and A_d/A_r. Five design points of interest are highlighted.

Of those diffuser-augmented turbines presented, 27 may be classified as 'low standard' and 25 as 'high standard.' Table 7.1 lists the usual traits of each of those types, where high standard traits can be taken as design suggestions for the interested reader.

Table 7.1 – Common traits of a low and high standard diffusers.

Common low standard traits
Conical diffusers
High A_d, resulting in lower evaluation in the current metric
Expansion angles smaller than 10 degrees
Sharp flow expansion, resulting in boundary layer separation
Addition of unnecessary, size increasing, parts
Rotor out of optimum position inside the diffuser
Low C_p^b for associated bare turbine
Large gaps between diffuser throat and rotor blade's tip

Common high standard traits
Curved diffusers
Well designed flange height
Geometry optimization
Rotor designed considering the diffuser
Expansion angle optimization
Compact design
Rotor positioned at the section which induces highest mass flow
High C_p^b of associated bare turbine

It is important to notice the lack of diffuser-augmented turbines on the top-right corner of Figure 7.4. Diffusers with A_d/A_r higher than 2.5 are more susceptible to flow separation and the creation of recirculation zones inside them. This phenomenon is independent of the expansion angle adopted and detrimental for the diffuser enhancement. A balance is needed on the diffuser's design to achieve optimal results.

Five diffuser designs are worth pointing out. Each one presented results beyond average and are compact in their designs, i.e., have high values of C_p^d and low A_d/A_r. They also show value in their adopted methodology, experimental procedures, or novelty of their designs.

- Design 1

  Oka et al. [113], in 2015, reported a diffuser design that goes beyond the power generation limit of bare wind turbines. This design is based on the simultaneous optimization of the aerodynamic of the rotor and a curved diffuser with flange.

They also published two other works that build-up to this method [112, 111]. In all three articles, they discuss their methods and the multi-objective genetic algorithm employed. The Pareto optimal solutions found are compared to wind-tunnel experimental data. Results show power coefficients values above those of the Betz limit for bare turbines, reaching a C_p^d of 0.62. However, it is important to note that the energy extraction limit, when applied for diffuser-augmented turbines, is different for each case, as explained in Chapter 4 [69].

The design presented by Oka et al. [113] lacks details on the methodology employed in the numerical analysis and experimental tests for the claims the article hold. However, the concept presented still holds ground. Therefore, the readers are pointed to design point 2: a more thorough and detailed numerical analysis of a similar methodology.

- Design 2

  Khamlaj and Rhumpfkeil [78], in 2018, also employed a multi-objective genetic algorithm to improve their rotor and diffuser design simultaneously. Their work was purely numerical, but with a broad explanation of the methodology. They also discuss the effects of drag on the structure based on different geometries, pointing in the direction of more compact diffuser designs as a priority.

  Figure 7.5(a) illustrates the design analysis, that had three parameters as a basis: power coefficient, thrust coefficient, and drag coefficient. The designs are classified by an objective function, where the objectively best are colored in black. Figure 7.5(b) illustrates one of the selected cases by the authors, Profile H (design point 2), that presented a C_p^d of 0.50.

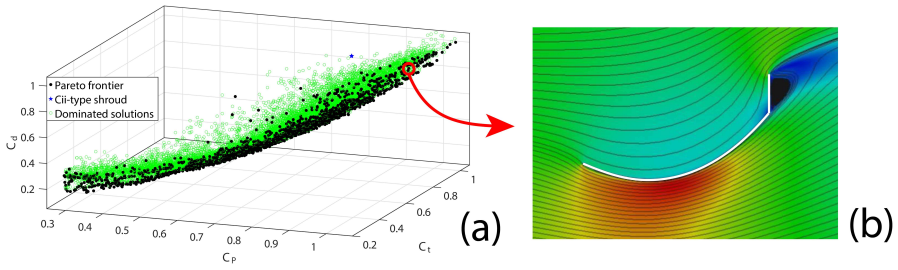

Figure 7.5 – Diffuser-augmented turbine optimization. Analyzed cases in (a), with objectively best ones in black. Selected profile H illustration in (b), referred as design point 2. Reused and edited with permission [78]

It is important to notice that all cases analyzed by the authors were of curved diffusers with flange. Several more opportunities exist to study several other shapes with the same technique.

- Design 3

  Heikal et al. [59], in 2018, developed a diffuser model based on the wind lens design [105]. They employed two concepts on their flanged design: flange inclination angle and inner flange depth. Results presented a C_p^d of 0.57, at a positive angle of 10 degrees, an improvement of 28% over the original lens *Cii* version. The TSR operation point also shifted to higher intervals of rotor rotation. Figure 7.6 shows the differences between the flow streamlines due to the flange inclination. It can be observed how the reversed flange angle shifted the diffuser flow expansion to a higher degree.

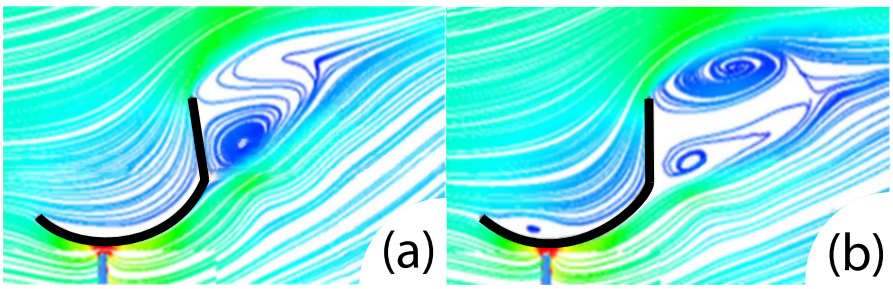

Figure 7.6 – Diffuser-augmented turbine with flange inclination. Flange with positive 10° angle in (a), referred design point 3, and 0° angle in (b). Reused and edited with permission [59].

- Design 4 and 5

  Ohya and Karasudani [105] proposed, in 2010, a series of diffuser designs, while studying flange height and their curve shape. Some of those designs are illustrated in Figure 7.7.

Figure 7.7 – Several diffuser-augmented turbines with varying lengths, experiments made with the same rotor [105]. Diffuser *C*0 - $0.100L/D_r$ in (a), *Ci* - $0.137L/D_r$ in (b), *Cii* - $0.221L/D_r$ in (c), *Ciii* - $0.371L/D_r$ in (d).

The diffuser shape *Cii*, with a flange height of $0.1D_r$, is pointed as the one with the highest performance. Through the analysis in terms of the C_p^d, more efficient and compact designs are preferred. The proposed *Ci* diffuser, design point 4, with flange height of $0.05D_r$, attained a C_p^d of 0.51. The proposed *C*0 diffuser, design point 5, with flange height of $0.05D_r$, attained a C_p^d of 0.49. In comparison, the reported *Cii* attained a C_p^d of 0.47. It is crucial to notice that an increase in flange height from 5% to 20% of the rotor diameter is impactful, especially when the diffuser design without flange has a diameter only 14% bigger than the rotor.

7.4 Diffuser enhancement

Diffusers are often designed as standalone projects from their rotors. Although not optimal, this method shows satisfactory results. Figure 7.8 relates the diffuser enhancement achieved, E_d, and the power coefficient, C_p^b, of their respective bare turbines.

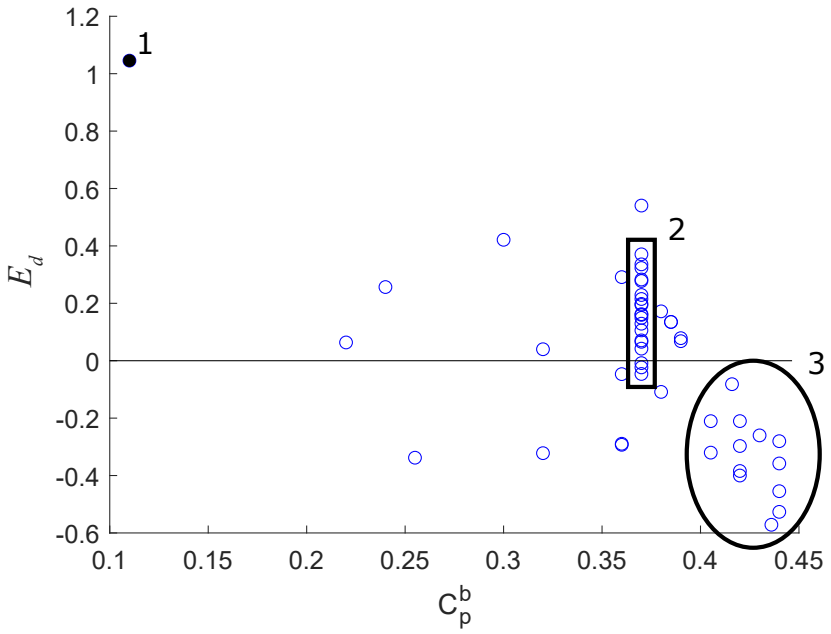

Figure 7.8 – Relation between the diffuser-enhancement achieved, E_d, and the power coefficient, C_p^b, of their respective bare turbines. Three areas of interest are highlighted.

Figure 7.8 shows three interesting areas to discuss. The first is the design point 1, illustrated by Figure 7.9, a diffuser design already mentioned in Section 7.1. Kosasih and Saleh [83], in 2016, designed a diffuser for a rotor with a power coefficient much lower than the standard, with a C_p^b of 0.11. The diffuser enhancement is noticeable, of 1.05, doubling the initial rotor power coefficient. Notwithstanding, the diffuser-augmented turbine's power coefficient, C_p^d, falls much lower than the average bare turbine's power coefficient, at 0.22.

Figure 7.9 – Conical diffuser-augmented turbine by Kosasih and Saleh [83].

Area number 2 is a series of experiments made by Ohya and Karasudani [105]. The series of experiments pointed in Area 2 were all made using the same rotor, testing it with different curved diffusers with flange, some of them illustrated in Figure 7.7. Since the starting point was the same C_p^b, it became evident how the diffuser design directly affects the diffuser enhancement. Since the criterion of analysis is E_d, the enhancement cannot be achieved by simply making a steeper contraption. This enhancement has to be implemented in a well planned and executed manner.

Area number 3 alerts us to be cautious when coupling a rotor of a high power coefficient with a diffuser. A common trend is observed: the lower the original turbine power coefficient, the easier it is to obtain a substantial diffuser enhancement; an extreme case being design point 1. On the other hand, rotors with a high power coefficient need a diffuser designed to be used with it to show any enhancement. To achieve the highest enhancement, planning the diffuser and rotor together is advised, as mentioned in Section 5.13.

8 Conclusions

A collection of 155 articles on diffuser-augmented horizontal-axis turbines was analyzed using a systematic approach to the literature. The work sample was classified into the 16 most prominent research branches. The most important findings in each of those branches were presented and discussed. As an addendum, research comparing the C_p^d of multi-slots diffusers with conventional ones at different A_d/A_r ratios, and of different multi-turbine arrangements on the same plane was identified as a promising avenue.

An evaluation of several diffuser-augmented turbines was carried out based on the actual power coefficient, C_p^d, taking into consideration the maximum cross-sectional area of the diffuser. To consider diffuser size and make a fair assumption on the diffuser-augmented turbine's worth, a power coefficient metric was proposed for inter-comparison: the diffuser-enhancement parameter, E_d. Population distribution of 60 diffuser-augmented turbines showed an average value of 0.75 on the maximum C_p, while an analysis based on the maximum C_p^d returned an average of 0.37. That points to a previous overestimation of the diffuser's worth. The diffuser-enhancement parameter was used to compare diffuser-augmented turbines to their bare turbines scaled to the same size. Data revealed that an enhancement happened on 58% of the diffuser-augmented turbines evaluated, where using a diffuser was the better option over making a bigger rotor. In terms of power conversion, a diffuser may enhance a turbine or be detrimental to it; on the proposed metrics, a diffuser's value depends entirely on design.

An analysis based on the tip-speed-ratio followed. To compare the diffuser-augmented turbine with its bare counterpart, two parameters were proposed: the shift in the optimum operation point, TSR^*_{center}, and the change in operation interval, TSR^*_{width}. Through the analysis, on 34 turbines, it was observable that diffusers tend to narrow the power coefficient curves, reducing their optimum operational interval.

Diffuser-augmented turbines were classified into two groups based on their C_p^d. The common traits of the high standard and low standard groups were presented. Five high achieving diffuser designs were pointed out with their most relevant achievements.

It was found that diffusers with $A_d/A_r > 2.5$ did not achieve high C_p^d. An analysis based on E_d revealed a trend that diffusers more easily improve bare turbines with lower power coefficient. Care is advised when using a diffuser on high-performance bare turbines; it is ideal to design the rotor and diffuser together, with previous forethought on the diffuser-augmented turbine.

Bibliography

[1] Andrew Grant Ã, Cameron Johnstone, Nick Kelly, A Grant, Cameron Johnstone, and Nick Kelly. Urban wind energy conversion: The potential of ducted turbines. *Renewable Energy*, 33(6):1157–1163, 2008. Citado 2 vezes nas páginas 24 and 38.

[2] K Abe, H Kihara, A Sakurai, E Wada, K Sato, M Nishida, and Y Ohya. An experimental study of tip-vortex structures behind a small wind turbine with a flanged diffuser. *Wind and Structures, An International Journal*, 9(5):413–417, 2006. Citado 2 vezes nas páginas 34 and 37.

[3] K Abe, M Nishida, A Sakurai, Y Ohya, H Kihara, E Wada, and K Sato. Experimental and numerical investigations of flow fields behind a small wind turbine with a flanged diffuser. *Journal of Wind Engineering and Industrial Aerodynamics*, 93(12):951–970, 2005. Citado 3 vezes nas páginas 24, 101, and 105.

[4] K Abe and Y Ohya. An investigation of flow fields around flanged diffusers using CFD. *Journal of Wind Engineering and Industrial Aerodynamics*, 92(3-4):315–330, 2004. Citado 2 vezes nas páginas 24 and 42.

[5] A Agha, H N Chaudhry, and F Wang. Diffuser Augmented Wind Turbine (DAWT) technologies: A review. *International Journal of Renewable Energy Research*, 8(3):1369–1385, 2018. Citado 2 vezes nas páginas 17 and 53.

[6] A Amer, A H H Ali, Y Elmahgary, and S Ookawara. Effect of diffuser configuration on the flow field pattern inside wind concentrator. In *1st International Renewable and Sustainable Energy Conference, IRSEC 2013*, pages 212–217, Department of Energy Resources and Environmental Engineering, Egypt-Japan University of Science and Technology, Alexandria, 21934, Egypt, 2013. Citado 2 vezes nas páginas 41 and 47.

[7] A Anzai, Y Nemoto, and I Ushiyama. Wind tunnel analysis of concentrators for augmented wind turbines. *Wind Engineering*, 28(5):605–614, 2004. Citado na página 47.

[8] A C Aranake and K Duraisamy. Aerodynamic optimization of shrouded wind turbines. *Wind Energy*, 20(5):877–889, 2017. Citado na página 33.

[9] Aniket C. Aranake, Vinod K. Lakshminarayan, and Karthik Duraisamy. Computational analysis of shrouded wind turbine configurations. In *51st AIAA Aerospace Sciences Meeting including the New Horizons Forum and Aerospace Exposition 2013*, Department of Aeronautics and Astronautics, Stanford University, Stanford, CA, United States, 2013. Citado na página 35.

[10] Aniket C. Aranake, Vinod K. Lakshminarayan, and Karthik Duraisamy. A assessment of low-order theories for analysis and design of shrouded wind turbines using CFD. In *5th Science of Making Torque from Wind Conference, TORQUE 2014*, volume 524, 496 Lomita Mall, Stanford, CA 94305, United States, 2014. Institute of Physics Publishing. Citado na página 25.

[11] Aniket C. Aranake, Vinod K. Lakshminarayan, and Karthik Duraisamy. Computational analysis of shrouded wind turbine configurations using a 3-dimensional RANS solver. *Renewable Energy*, 75:818–832, 2015. Citado 2 vezes nas páginas 25 and 35.

[12] F Avallone, D Casalino, and D Ragni. On the effect of the tip clearance on the aerodynamic and aeroacoustics of a diffuser-augmented wind turbine. In *AIAA Scitech Forum, 2019*, Delft University of Technology, Department of Aerodynamic, Wind Energy and Propulsion, Kluyverweg 1, Delft, 2629HS, Netherlands, 2019. American Institute of Aeronautics and Astronautics Inc, AIAA. Citado na página 34.

[13] F Avallone, D Ragni, and D Casalino. On the effect of the tip-clearance ratio on the aeroacoustics of a diffuser-augmented wind turbine. *Renewable Energy*, 152:1317–1327, 2020. Citado na página 34.

[14] Ralph-peter Bailey. Vortex enhanced wind turbine diffuser, May 2012. Citado na página 53.

[15] F Baratchi, T L Jeans, and A G Gerber. A modified implementation of actuator line method for simulating ducted tidal turbines. *Ocean Engineering*, 193, 2019. Citado na página 32.

[16] F. Baratchi, T.L. L Jeans, and A.G. G Gerber. Assessment of blade element actuator disk method for simulations of ducted tidal turbines. *Renewable Energy*, 154:290–304, 2020. Citado na página 33.

[17] Albert Betz. *Introduction to the theory of flow machines*. Elsevier, 1966. Citado na página 29.

[18] R. Bontempo and M. Manna. Solution of the flow over a non-uniform heavily loaded ducted actuator disk. *Journal of Fluid Mechanics*, 2013. Citado na página 32.

[19] R Bontempo and M. Manna. Performance analysis of open and ducted wind turbines. *Applied Energy*, 136:405–416, 2014. Citado 2 vezes nas páginas 25 and 32.

[20] R Bontempo and M. Manna. Effects of the duct thrust on the performance of ducted wind turbines. *Energy*, 99:274–287, 2016. Citado 2 vezes nas páginas 25 and 32.

[21] R. Bontempo and M. Manna. On the potential of the ideal diffuser augmented wind turbine: an investigation by means of a momentum theory approach and of a free-wake ring-vortex actuator disk model. *Energy Conversion and Management*, 213, 2020. Citado na página 33.

[22] Bridget Buehrle, Ravi A Kishore, and Shashank Priya. Computational modeling of ducted wind turbines for residential applications. In *ASME 2013 International Mechanical Engineering Congress and Exposition, IMECE 2013*, volume 6 A, pages 1–10, CEHMS, Virginia Tech, Blacksburg, VA, United States, 2013. American Society of Mechanical Engineers (ASME). Citado na página 41.

[23] Tony Burton, Nick Jenkins, David Sharpe, and Ervin Bossanyi. *Wind Energy Handbook, Second Edition*. 2011. Citado na página 31.

[24] C Cardona-Mancilla, J.S.-D. Rio, D Hincapié-Zuluaga, and E Chica. A numerical simulation of horizontal axis hydrokinetic turbine with and without augmented diffuser. *International Journal of Renewable Energy Research*, 8(4):1833–1839, 2018. Citado 2 vezes nas páginas 98 and 102.

[25] Rym Chaker, Mouldi Kardous, Mahmoud Chouchen, Fethi Aloui, Sassi Ben Nasrallah, and Sassi Ben Nasrallah. Vortices' Characteristics to Explain the Flange Height Effects on the Aerodynamic Performances of a Diffuser Augmented Wind Turbine. *Journal of Solar Energy Engineering, Transactions of the ASME*, 138(6):061013, 2016. Citado 3 vezes nas páginas 9, 42, and 43.

[26] Su Huei S.-H. Chang, Q.-H. Qi Hong Lim, and K.-H. Kuo Hsin K.-H. Lin. Design of a wind energy capturing device for a vehicle. In Al-Dabass D., Sauli Z., and Zakaria Z., editors, *5th International Conference on Intelligent Systems, Modelling and Simulation, ISMS 2014*, volume 2015-Septe, pages 435–440, Department of Industrial Education, National Taiwan Normal University, Taipei, Taiwan, 2015. IEEE Computer Society. Citado 2 vezes nas páginas 99 and 103.

[27] T. Y. Chen, C. W. Hung, and Y. T. Liao. Experimental study on aerodynamics of micro-wind turbines with large-tip non-twisted blades. *Journal of Mechanics*, 29(3):N15–N20, 2012. Citado 4 vezes nas páginas 99, 100, 103, and 104.

[28] E Chica, F Pérez, and A Rubio-Clemente. Influence of the diffusor angle and a damper opening angle on the performance of a hydrokinetic turbine. *Environmental Progress and Sustainable Energy*, 37(2):824–831, 2018. Citado 2 vezes nas páginas 98 and 102.

[29] Souma Chowdhury, Jie Zhang, Achille Messac, and Luciano Castillo. Optimizing the arrangement and the selection of turbines for wind farms subject to varying wind conditions. *Renewable Energy*, 2013. Citado na página 50.

[30] G Civalier, C Fridley, J Li, J Seabe, A.-X. Stanciu, M Willey, and R S Pant. Comparative analysis of three concepts for Aerostat based electrical power generation system. In *11th AIAA Aviation Technology, Integration, and Operations (ATIO) Conference, including the AIAA Balloon Systems Conference and 19th AIAA Lighter-Than-Air Technology Conference 2011*, Virginia Polytechnic Institute and

State University, Aerospace and Ocean Engineering Department, Blacksburg, VA, 24061, United States, 2011. Citado na página 36.

[31] D P Coiro, G Troise, F Scherillo, A. De Marco, G. Calise, and N. Bizzarrini. Development, deployment and experimental test on the novel tethered system GEM for tidal current energy exploitation. *Renewable Energy*, 114:323–336, 2017. Citado 3 vezes nas páginas 53, 98, and 102.

[32] Domenico P. Coiro, Elia Daniele, and Pierluigi Della Vecchia. Diffuser shape optimization for GEM, a tethered system based on two horizontal axis hydro turbines. *International Journal of Marine Energy*, 13:169–179, 2016. Citado 3 vezes nas páginas 36, 98, and 102.

[33] John T. Conway. Exact actuator disk solutions for non-uniform heavy loading and slipstream contraction. *Journal of Fluid Mechanics*, 1998. Citado na página 32.

[34] Patricia Cronin, Frances Ryan, and Michael Coughlan. Undertaking a literature review: a step-by-step approach. *British Journal of Nursing*, 17(1):38–43, 2008. Citado na página 18.

[35] E Daniele and D P Coiro. Optimization of diffuser geometry for an horizontal axis shrouded hydro turbine. In *4th International Conference on Clean Electrical Power: Renewable Energy Resources Impact, ICCEP 2013*, pages 240–247, Department of Industrial Engineering - Aerospace Section, Università degli Studi di Napoli Federico II, Via Claudio 21, 80125, Napoli, Italy, 2013. Citado na página 36.

[36] E Daniele, E Ferrauto, and D P Coiro. Horizontal axis hydroturbine shroud airfoil optimization. In Greiner D., Galvan B., Winter G., Gauger N., Periaux J., Periaux J., and Giannakoglou K., editors, *10th International Conference on Advances in Evolutionary and Deterministic Methods for Design, Optimization and Control in Engineering and Sciences, 2013*, volume 36, pages 241–256, Ammerländer, Heerstraße 136, Oldenburg, 26129, Germany, 2015. Springer Netherland. Citado na página 36.

[37] O de Vries. Fluid dynamic aspects of wind energy conversion. *AGARDograph*, (243):148, 1979. Citado na página 31.

[38] V V Dighe, F Avallone, J Tang, and G J W van Bussel. Effects of gurney flap on the performance of diffuser augmented wind turbines. In *35th Wind Energy Symposium, 2017*, Wind Energy Research Group, Delft University of Technology, Delft, 2629HS, Netherlands, 2017. American Institute of Aeronautics and Astronautics Inc, AIAA. Citado na página 42.

[39] V V Dighe, F Avallone, G Van Bussel, and O Igra. Multi-element ducts for ducted wind turbines: A numerical study. *Wind Energy Science*, 4(3):439–449, 2019. Citado 2 vezes nas páginas 33 and 48.

[40] V V Dighe, F Avallone, and G J W van Bussel. Computational study of diffuser augmented wind turbine using actuator disc force method. *International Journal of Computational Methods and Experimental Measurements*, 4(4):522–531, 2016. Citado na página 33.

[41] V V Dighe, G de Oliveira, F Avallone, and G J W van Bussel. On the effects of the shape of the duct for ducted wind turbines. In *Wind Energy Symposium, 2018*, number 210029, Wind Energy Research Group, Delft University of Technology, Delft, 2629HS, Netherlands, 2018. American Institute of Aeronautics and Astronautics Inc, AIAA. Citado 2 vezes nas páginas 8 and 40.

[42] Vinit V Dighe, Francesco Avallone, and Gerard van Bussel. Effects of yawed inflow on the aerodynamic and aeroacoustic performance of ducted wind turbines. *Journal of Wind Engineering and Industrial Aerodynamics*, 201(November 2019):104174, 2020. Citado na página 34.

[43] D.A.T.D. do Rio Vaz, André Luiz Amarante Mesquita, J R P Vaz, Claudio José Cavalcante Blanco, João Tavares Pinho, Déborah Aline Tavares Dias Do Rio Vaz, André Luiz Amarante Mesquita, Jerson Rogério Pinheiro Vaz, Claudio José Cavalcante Blanco, João Tavares Pinho, D.A.T.D. do Rio Vaz, André Luiz Amarante Mesquita, J R P Vaz, Claudio José Cavalcante Blanco, and João Tavares Pinho. An extension of the Blade Element Momentum method applied to Diffuser Augmented Wind Turbines. *Energy Conversion and Management*, 87:1116–1123, 2014. Citado na página 32.

[44] Aly M. El-Zahaby, A. E. Kabeel, S. S. Elsayed, and M. F. Obiaa. CFD analysis of flow fields for shrouded wind turbine's diffuser model with different flange angles. *Alexandria Engineering Journal*, 56(1):171–179, 2017. Citado na página 43.

[45] Elsevier. Scopus content coverage guide. Retrieved from https://www.elsevier.com/?a=69451, August 29, 2020. Citado na página 18.

[46] Elsevier. Scopus [database], 2004. Retrieved from https://scopus.com, August 29, 2020. Citado na página 18.

[47] Clive A.J. J Fletcher. Computational analysis of diffuser-augmented wind turbines. *Energy Conversion and Management*, 21(3):175–183, 1981. Citado 3 vezes nas páginas 35, 101, and 105.

[48] Tudor Foote and Ramesh K Agarwal. Optimization of power generation from shrouded wind turbines. In *ASME 2012 6th International Conference on Energy Sustainability, ES 2012, Collocated with the ASME 2012 10th International Conference on Fuel Cell Science, Engineering and Technology*, number PARTS A AND B, pages 1325–1331, Department of Engineering, Washington University, Saint Louis, MO, United States, 2012. American Society of Mechanical Engineers. Citado na página 41.

[49] K M Foreman, B L Gilbert, and R A Oman. Diffuser augmentation of wind turbines. *Solar Energy*, 20(4):305–311, 1978. Citado 2 vezes nas páginas 24 and 31.

[50] D L F Gaden and E L Bibeau. A numerical investigation into the effect of diffusers on the performance of hydro kinetic turbines using a validated momentum source turbine model. *Renewable Energy*, 35(6):1152–1158, 2010. Citado 2 vezes nas páginas 25 and 32.

[51] B L Gilbert and K M Foreman. Experiments with a diffuser-augmented model wind turbine. *Journal of Energy Resources Technology, Transactions of the ASME*, 105(1):46–53, 1983. Citado na página 24.

[52] Barry L Gilbert, Richard A Oman, and Kenneth M Foreman. FLUID DYNAMICS OF DIFFUSER-AUGMENTED WIND TURBINES. *J Energy*, 2(6):368–374, 1978. Citado na página 31.

[53] L. A. Gish and G. Hawbaker. Experimental and numerical study on performance of shrouded hydrokinetic turbines. In *2016 OCEANS MTS/IEEE Monterey, OCE 2016*, Department of Naval Architecture and Ocean Engineering, United States Naval Academy, Annapolis, MD, United States, 2016. Institute of Electrical and Electronics Engineers Inc. Citado 2 vezes nas páginas 98 and 102.

[54] Uli Göltenbott, Yuji Ohya, Shigeo Yoshida, and Peter Jamieson. Aerodynamic interaction of diffuser augmented wind turbines in multi-rotor systems. *Renewable Energy*, 112:25–34, 2017. Citado na página 50.

[55] A Grant and N Kelly. A ducted wind turbine model for building simulation. *Building Services Engineering Research and Technology*, 25(4):339–349, 2004. Citado na página 38.

[56] Daniel Gysling and Ercan Dumlupinar. Mixer-ejector turbine with annular airfoils, June 2014. Flodesign Wind Turbine Corp. Citado 2 vezes nas páginas 9 and 48.

[57] Wanlong Wanjin Han, Peigang Yan, Wanlong Wanjin Han, and Yurong He. Design of wind turbines with shroud and lobed ejectors for efficient utilization of low-grade wind energy. *Energy*, 89:687–701, 2015. Citado 4 vezes nas páginas 9, 45, 101, and 105.

[58] I. Hashem, M. H. Mohamed, and A. A. Hafiz. Aero-acoustics noise assessment for Wind-Lens turbine. *Energy*, 2017. Citado na página 33.

[59] Hasim A. Heikal, Osayed S.M. M Abu-Elyazeed, Mohamed A.A. A Nawar, Youssef A. Attai, and Maged M.S. S Mohamed. On the actual power coefficient by theoretical developing of the diffuser flange of wind-lens turbine. *Renewable Energy*, 125:295–305, 2018. Citado 5 vezes nas páginas 10, 43, 67, 98, and 102.

[60] Y G Heo, N J Choi, K H Choi, H S Ji, and K C Kim. CFD study on aerodynamic power output of a 110 kW building augmented wind turbine. *Energy and Buildings*, 129:162–173, 2016. Citado na página 38.

[61] Hermawan, M. A. Bramantya, Nur Kholis Majid, and Andre Febrianto. Experimental study effect of flange addition on mechanical power of diffuser augmented counter rotating wind turbine. In Hohne T., Pranoto I., Deendarlianto, Majid A.I., Wiranata A., Widyaparaga A., and Takei M., editors, *9th International Conference on Thermofluids 2017, THERMOFLUID 2017*, volume 2001, pages 3–10, Mechanical and Industrial Department, Universtias Gadjah Mada Yogyakarta, Indonesia, 2018. American Institute of Physics Inc. Citado na página 42.

[62] D. A. Howey, A. Bansal, and A. S. Holmes. Design and performance of a centimetre-scale shrouded wind turbine for energy harvesting. *Smart Materials and Structures*, 20(8), 2011. Citado 2 vezes nas páginas 24 and 25.

[63] J.-F. Hu and W.-X. Wang. Upgrading a shrouded wind turbine with a self-adaptive flanged diffuser. *Energies*, 8(6):5319–5337, 2015. Citado na página 43.

[64] O Igra. Research and development for shrouded wind turbines. *Energy Conversion and Management*, 21(1):13–48, 1981. Citado na página 53.

[65] O Igra. Shrouded wind turbine research in Israel. *International Journal of Ambient Energy*, 2(2):85–96, 1981. Citado 3 vezes nas páginas 24, 48, and 53.

[66] Ozer Igra. The shrouded aerogenerator. *Energy*, 2(4):429–439, 1977. Citado na página 53.

[67] S. A H Jafari, B. Kosasih, P B Kosasih, B. Kosasih, P B Kosasih, and B. Kosasih. Flow analysis of shrouded small wind turbine with a simple frustum diffuser with computational fluid dynamics simulations. *Journal of Wind Engineering and Industrial Aerodynamics*, 125:102–110, 2014. Citado 2 vezes nas páginas 25 and 42.

[68] Peter Jamieson. Generalized limits for energy extraction in a linear constant velocity flow field. *Wind Energy*, 11(5):445–457, 2008. Citado 2 vezes nas páginas 31 and 32.

[69] Peter M. Jamieson. Beating Betz: Energy Extraction Limits in a Constrained Flow Field. *Journal of Solar Energy Engineering-transactions of The Asme - J SOL*

ENERGY ENG, 131(3):0310081–0310086, 8 2009. Citado 3 vezes nas páginas 29, 31, and 66.

[70] S A Kale, Y R Gunjal, S P Jadhav, and A N Tanksale. CFD analysis for optimization of diffuser for a micro wind turbine. In *2013 International Conference on Energy Efficient Technologies for Sustainability, ICEETS 2013*, pages 257–260, Mechanical Engineering Department, Trinity College of Engineering and Research, Pune, India, 2013. Citado na página 43.

[71] Benjamin Kanya and Kenneth D. Visser. Experimental validation of a ducted wind turbine design strategy. *Wind Energy Science*, 2018. Citado 2 vezes nas páginas 9 and 48.

[72] M Kardous, R Chaker, F Aloui, and I Abidi. Locations of vortices and their impacts on the aerodynamic performances of a diffuser and a DAWT. In *3rd International Conference on Renewable Energies for Developing Countries, REDEC 2016*, Laboratory of Wind Energy Management and Waste Energy Recovery, LMEEVED, Research and Technology Center of Energy, Borj Cedria Technopark, Tunis, Tunisia, 2016. Institute of Electrical and Electronics Engineers Inc. Citado na página 43.

[73] M. Kardous, R. Chaker, F. Aloui, and S. Ben Nasrallah. On the dependence of an empty flanged diffuser performance on flange height: Numerical simulations and PIV visualizations. *Renewable Energy*, 56:123–128, 2013. Citado na página 43.

[74] S Ke, W Wen-Quan, and Y Yan. The hydrodynamic performance of a tidal-stream turbine in shear flow. *Ocean Engineering*, 199, 2020. Citado na página 53.

[75] Nemat Keramat Siavash, G. Najafi, Teymour Tavakkoli Hashjin, Barat Ghobadian, and Esmail Mahmoodi. An innovative variable shroud for micro wind turbines. *Renewable Energy*, 145:1061–1072, 2020. Citado na página 48.

[76] T A Khamlaj and M P Rumpfkeil. Analysis and optimization study of shrouded horizontal axis wind turbines. In *Wind Energy Symposium, 2018*, number 210029, Dept. of Mechanical and Aerospace Eng., University of Dayton, Dayton, OH 45469-0238, United States, 2018. American Institute of Aeronautics and Astronautics Inc, AIAA. Citado na página 51.

[77] Tariq Abdulsalam Khamlaj and Markus Peer Rumpfkeil. Theoretical analysis of shrouded horizontal axis wind turbines. *Energies*, 10(1):1–19, 2017. Citado 2 vezes nas páginas 32 and 51.

[78] Tariq Abdulsalam Khamlaj and Markus Peer Rumpfkeil. Analysis and optimization of ducted wind turbines. *Energy*, 162:1234–1252, 2018. Citado 8 vezes nas páginas 9, 10, 42, 51, 66, 67, 101, and 105.

[79] Ravi Anant Kishore, Thibaud Coudron, and Shashank Priya. Small-scale wind energy portable turbine (SWEPT). *Journal of Wind Engineering and Industrial Aerodynamics*, 116:21–31, 2013. Citado na página 25.

[80] E Koç and T Yavuz. Effect of flap on the wind turbine-concentrator combination. *International Journal of Renewable Energy Research*, 9(2):551–560, 2019. Citado na página 48.

[81] B Kosasih, S A H Jafari, P B Kosasih, S A H Jafari, B Kosasih, S A H Jafari, P B Kosasih, S A H Jafari, B Kosasih, and S A H Jafari. High-efficiency shrouded micro wind turbine for urban-built environment. In *International Conference on Mechanical Engineering, ICOME 2013*, volume 493, pages 294–299, School of Mechanical, Materials and Mechatronics Engineering, University of Wollongong, NSW 2500, Australia, 2014. Citado na página 25.

[82] Buyung Kosasih, Andrea Tondelli, P B Kosasih, and Andrea Tondelli. Experimental study of shrouded micro-wind turbine. In *Evolving Energy-International Energy Foundation International Energy Congress, IEF-IEC 2012*, volume 49, pages 92–98, School of Mechanical, Materials and Mechatronics Engineering, University of Wollongong, Northfields Ave., Wollongong, NSW 2522, Australia, 2012. Elsevier Ltd. Citado 5 vezes nas páginas 42, 47, 52, 99, and 103.

[83] P B Kosasih, H. Saleh Hudin, B. Kosasih, H. Saleh Hudin, P B Kosasih, H. Saleh Hudin, B. Kosasih, and H. Saleh Hudin. Influence of inflow turbulence intensity on the performance of bare and diffuser-augmented micro wind turbine model. *Renewable Energy*, 87:154–167, 2016. Citado 6 vezes nas páginas 10, 61, 69, 70, 99, and 103.

[84] M Kulak, M Karczewski, K Olasek, and K Jóźwik. CFD analysis of Diffuser Augmented Wind Turbine model for wind tunnel investigation. In *42nd Conference of the Industrial Electronics Society, IECON 2016*, pages 5538–5543, Institute of Turbomachinery, Faculty of Mechanical Engineering, Lodz University of Technology, Łódź, Poland, 2016. IEEE Computer Society. Citado na página 43.

[85] Vedant Kumar and Sandeep Saha. Theoretical performance estimation of shrouded-twin-rotor wind turbines using the actuator disk theory. *Renewable Energy*, 134:961–969, 2019. Citado 2 vezes nas páginas 33 and 52.

[86] Jim Y.J. Kuo, David A. Romero, J. Christopher Beck, and Cristina H. Amon. Wind farm layout optimization on complex terrains – Integrating a CFD wake model with mixed-integer programming. *Applied Energy*, 178:404–414, 2016. Citado na página 50.

[87] C. J. Lawn. Optimization of the power output from ducted turbines. *Proceedings of the Institution of Mechanical Engineers, Part A: Journal of Power and Energy*, 217(1):107–118, 2003. Citado 3 vezes nas páginas 24, 31, and 32.

[88] S N Leloudas, G N Lygidakis, A I Eskantar, and I K Nikolos. A robust methodology for the design optimization of diffuser augmented wind turbine shrouds. *Renewable Energy*, 150:722–742, 2020. Citado na página 36.

[89] G M Lilley and W J Rainbird. A Preliminary Report on the Design and Performance of a Ducted Windmill. Technical report, 1956. Citado 2 vezes nas páginas 30 and 31.

[90] M Lipian, I Dobrev, M Karczewski, F Massouh, and K Jozwik. Small wind turbine augmentation: Experimental investigations of shrouded- and twin-rotor wind turbine systems. *Energy*, 186, 2019. Citado na página 52.

[91] M. Lipian, I. Dobrev, F. Massouh, and K. Jozwik. Small wind turbine augmentation: Numerical investigations of shrouded- and twin-rotor wind turbines. *Energy*, 201, 2020. Citado 2 vezes nas páginas 37 and 52.

[92] Michał Lipian, Maciej Karczewski, and Krzysztof Olasek. Sensitivity study of diffuser angle and brim height parameters for the design of 3 kW Diffuser Augmented Wind Turbine. *Open Engineering*, 5(1):280–286, 2015. Citado na página 43.

[93] Y Liu and S Yoshida. An extension of the Generalized Actuator Disc Theory for aerodynamic analysis of the diffuser-augmented wind turbines. *Energy*, 93:1852–1859, 2015. Citado na página 32.

[94] A. L. Loeffler, A L Loeffler Jr., A L Loeffler Jr., and A L Loeffler Jr. Flow field analysis and performance of wind turbines employing slotted diffusers. *Journal of Solar Energy Engineering, Transactions of the ASME*, 103(1):17–22, 1981. Citado na página 48.

[95] A. Mariotti, G. Buresti, and M. V. Salvetti. Use of multiple local recirculations to increase the efficiency in diffusers. *European Journal of Mechanics, B/Fluids*, 50:27–37, 2015. Citado na página 53.

[96] P.-M. Masukume, G Makaka, and P Mukumba. Optimization of the power output of a bare wind turbine by the use of a plain conical diffuser. *Sustainability (Switzerland)*, 10(8), 2018. Citado 2 vezes nas páginas 98 and 102.

[97] Toshio Matsushima, Shinya Takagi, and Seiichi Muroyama. Characteristics of a highly efficient propeller type small wind turbine with a diffuser. *Renewable Energy*, 31(9):1343–1354, 2006. Citado 3 vezes nas páginas 24, 41, and 42.

[98] N Mehmood, Z Liang, and J Khan. Diffuser augmented horizontal axis tidal current turbines. *Research Journal of Applied Sciences, Engineering and Technology*, 4(18):3522–3532, 2012. Citado na página 36.

[99] Nasir Mehmood, Zhang Liang, and Jawad Khan. CFD study of NACA 0018 for diffuser design of tidal current turbines. *Research Journal of Applied Sciences, Engineering and Technology*, 4(21):4552–4560, 2012. Citado na página 36.

[100] S Mertens. Wind energy in urban areas: Concentrator effects for wind turbines close to buildings. *Refocus*, 3(2):22–24, 2002. Citado na página 38.

[101] L Michal, K Maciej, and J Krzysztof. Analysis and comparison of numerical methods for design and development of small Diffuser-Augmented Wind Turbine (DAWT). In *42nd Conference of the Industrial Electronics Society, IECON 2016*, pages 5525–5531, Institute of Turbomachinery, Lodz University of Technology, Lodz, Poland, 2016. IEEE Computer Society. Citado na página 32.

[102] Lipian Michał, Karczewski MacIej, Molinski Jakub, Jozwik Krzysztof, L Michal, Karczewski MacIej, Molinski Jakub, Jozwik Krzysztof, Lipian Michał, Karczewski MacIej, Molinski Jakub, Jozwik Krzysztof, L Michal, Karczewski MacIej, Molinski Jakub, Jozwik Krzysztof, Lipian Michał, Karczewski MacIej, Molinski Jakub, and Jozwik Krzysztof. Numerical simulation methodologies for design and development of Diffuser-Augmented Wind Turbines-analysis and comparison. *Open Engineering*, 6(1):235–240, 2016. Citado na página 32.

[103] Aulia Nasution and Deka Wahyu Purwanto. Optimized curvature interior profile for Diffuser Augmented Wind Turbine (DAWT) to increase its energy-conversion performance. In *2011 IEEE 1st Conference on Clean Energy and Technology, CET 2011*, pages 315–320, Dept. of Engineering Physics, Faculty of Industrial Technology, Institut Teknologi Sepuluh Nopember (ITS) Surabaya, Sukolilo Surabaya 60111, Indonesia, 2011. Citado na página 40.

[104] M M Nunes, R C F Mendes, T F Oliveira, and A C P Brasil Junior. An experimental study on the diffuser-enhanced propeller hydrokinetic turbines. *Renewable Energy*, 133:840–848, 2019. Citado 4 vezes nas páginas 9, 57, 98, and 102.

[105] Y Ohya and T Karasudani. A shrouded wind turbine generating high output power with wind-lens technology. *Energies*, 3(4):634–649, 2010. Citado 14 vezes nas páginas 10, 24, 25, 33, 40, 41, 42, 67, 68, 70, 100, 101, 104, and 105.

[106] Y Ohya, T Karasudani, A Sakurai, K.-i. Abe, and M Inoue. Development of a shrouded wind turbine with a flanged diffuser. *Journal of Wind Engineering and Industrial Aerodynamics*, 96(5):524–539, 2008. Citado na página 24.

[107] Y Ohya, T Uchida, T Karasudani, M Hasegawa, and H Kume. Numerical studies of flow around a wind turbine equipped with a flanged-diffuser shroud using an

actuator-disk model. *Wind Engineering*, 36(4):455–472, 2012. Citado na página 33.

[108] Yuji Ohya. Bluff body flow and vortex - Its application to wind turbines. *Fluid Dynamics Research*, 46(6):61423, 2014. Citado 5 vezes nas páginas 9, 34, 44, 99, and 103.

[109] Yuji Ohya, Takashi Karasudani, Akira Sakurai, and Masahiro Inoue. Development of a high-performance wind turbine equipped with a brimmed diffuser shroud. *Transactions of the Japan Society for Aeronautical and Space Sciences*, 49(163):18–24, 2006. Citado na página 41.

[110] Yuji Ohya, Jumpei Miyazaki, Uli Göltenbott, and Koichi Watanabe. Power Augmentation of Shrouded Wind Turbines in a Multirotor System. *Journal of Energy Resources Technology, Transactions of the ASME*, 139(5), 2017. Citado na página 50.

[111] N Oka, M Furukawa, K Yamada, K Kawamitsu, K Kido, and A Oka. Simultaneous optimization of rotor blade and wind-lens for aerodynamic design of wind-lens turbine. In *ASME Turbo Expo 2014: Turbine Technical Conference and Exposition, GT 2014*, volume 3B, Department of Mechanical Engineering, Kyushu University, Fukuoka, Japan, 2014. American Society of Mechanical Engineers (ASME). Citado 2 vezes nas páginas 51 and 66.

[112] N Oka, M Furukawa, K Yamada, and K Kido. Aerodynamic design for wind-lens turbine using optimization technique. In *ASME 2013 Fluids Engineering Division Summer Meeting, FEDSM 2013*, volume 1 A, Department of Mechanical Engineering, Kyushu University, Fukuoka, Japan, 2013. Citado 2 vezes nas páginas 51 and 66.

[113] Nobuhito Oka, Masato Furukawa, Kazutoyo Yamada, Akihiro Oka, and Yasushi Kurokawa. Aerodynamic performances and flow fields of pareto optimal solutions in an aerodynamic design of a wind-lens turbine. In *ASME Turbo Expo 2015: Turbine Technical Conference and Exposition, GT 2015*, volume 9, Department of Mechanical Engineering, Kyushu University, Fukuoka, Japan, 2015. American

Society of Mechanical Engineers (ASME). Citado 7 vezes nas páginas 51, 60, 61, 65, 66, 99, and 103.

[114] C. B. Okhio, H. P. Horton, and G. Langer. Effects of swirl on flow separation and performance of wide angle diffusers. *International Journal of Heat and Fluid Flow*, 4(4):199, 1983. Citado na página 53.

[115] Krzysztof Olasek, Maciej Karczewski, Michal Lipian, Piotr Wiklak, Krzysztof Józwik, and K Józwik. Wind tunnel experimental investigations of a diffuser augmented wind turbine model. *International Journal of Numerical Methods for Heat and Fluid Flow*, 26(7):2033–2047, 2016. Citado 3 vezes nas páginas 43, 98, and 102.

[116] R A Oman, K M Foreman, and B L Gilbert. Investigation of diffuser-argumented wind turbines. Part II. Technical report, 1977. Citado 2 vezes nas páginas 31 and 48.

[117] Regina Negri Pagani, João Luiz Kovaleski, and Luis Mauricio Resende. Methodi Ordinatio: a proposed methodology to select and rank relevant scientific papers encompassing the impact factor, number of citation, and year of publication. *Scientometrics*, 105(3):2109–2135, 2015. Citado na página 18.

[118] D Petković, S Shamshirband, T Ćojbašić, V Nikolić, N B Anuar, A Q M Sabri, and S Akib. Adaptive neuro-fuzzy estimation of building augmentation of wind turbine power. *Computers and Fluids*, 97:188–194, 2014. Citado na página 39.

[119] D. G. Phillips, R. G.J. J Flay, and T. A. Nash. Aerodynamic analysis and monitoring of the Vortec 7 diffuser-augmented wind turbine. *Transactions of the Institution of Professional Engineers New Zealand. Electrical, Mechanical, and Chemical Engineering Section*, 26(1):13–19, 1999. Citado na página 48.

[120] D. G. Phillips, T. A. Nash, A. Oakey, R. G.J. J Flay, and P. J. Richards. Computational fluid dynamic and wind tunnel modelling of a Diffuser Augmented Wind Turbine. *Wind Engineering*, 23(1):7–13, 1999. Citado 2 vezes nas páginas 101 and 105.

[121] L. Prabhu, S. Prakash, Praveen Aadithya, Yoga Vignesh, and Sesha Rajakumaran. CFD analysis of shrouded diffuser wind turbine. *International Journal of Engineering and Advanced Technology*, 8(6 Special Issue 3):2100–2104, 2019. Citado na página 48.

[122] Walter M. Presz Jr. and Michael J. Werle. Wind turbine with mixers and ejectors, September 2011. Flodesign Wind Turbine Corp. Citado na página 53.

[123] Walter M. Presz Jr. and Michael J. Werle. Wind turbine with scalloped lobes, July 2011. Flodesign Wind Turbine Corp. Citado 2 vezes nas páginas 9 and 45.

[124] M H Ranjbar, S A Nasrazadani, and K Gharali. Optimization of a Flanged DAWT Using a CFD Actuator Disc Method. In Kunze H., Kilgour D.M., Makarov R., Melnik R., and Wang X., editors, *International conference on Applied Mathematics, Modeling and Computational Science, AMMCS 2017*, volume 259, pages 219–228, Faculty of Engineering, College of Mechanical Engineering, University of Tehran, Tehran, Iran, 2018. Springer New York LLC. Citado 2 vezes nas páginas 98 and 102.

[125] J Riglin, C Daskiran, N Oblas, W Chris Schleicher, and A Oztekin. Design and characteristics of a micro-hydrokinetic turbine system. In *ASME 2015 International Mechanical Engineering Congress and Exposition, IMECE 2015*, volume 6A-2015, P.C. Rossin College of Engineering and Applied Science, Lehigh University, Bethlehem, PA 18015, United States, 2015. American Society of Mechanical Engineers (ASME). Citado na página 63.

[126] J Riglin, W C Schleicher, and A Oztekin. Diffuser optimization for a micro-hydrokinetic turbine. In *ASME 2014 International Mechanical Engineering Congress and Exposition, IMECE 2014*, volume 7, P.C. Rossin College of Engineering and Applied Science, Lehigh University, Bethlehem, PA 18015, United States, 2014. American Society of Mechanical Engineers (ASME). Citado 3 vezes nas páginas 63, 99, and 103.

[127] Jacob Riglin, W. Chris Schleicher, and Alparslan Oztekin. Numerical analysis of a shrouded micro-hydrokinetic turbine unit. *Journal of Hydraulic Research*, 53(4):525–531, 2015. Citado 3 vezes nas páginas 63, 99, and 103.

[128] M Rowell, M Wosnik, J Barnes, and J P King. Experimental evaluation of a mixer-ejector marine hydrokinetic turbine at two open-water tidal energy test sites in NH and MA. *Marine Technology Society Journal*, 47(4):67–79, 2013. Citado na página 48.

[129] A Saleem and M.-H. Kim. Effect of rotor tip clearance on the aerodynamic performance of an aerofoil-based ducted wind turbine. *Energy Conversion and Management*, 201, 2019. Citado na página 37.

[130] F Scherillo, U Maisto, G Troise, D P Coiro, and S Miranda. Numerical and experimental analysis of a shrouded hydroturbine. In *3rd International Conference on Clean Electrical Power: Renewable Energy Resources Impact, ICCEP 2011*, pages 216–222, Dipartimento di Ingegneria Aerospaziale, Università degli Studi di Napoli Federico II, Italy, 2011. Citado 3 vezes nas páginas 53, 98, and 102.

[131] T Setoguchi, N Shiomi, and K Kaneko. Development of two-way diffuser for fluid energy conversion system. *Renewable Energy*, 29(10):1757–1771, 2004. Citado na página 43.

[132] Mohammad Shahsavarifard, E L Bibeau, and Vijay Chatoorgoon. Effect of shroud on the performance of horizontal axis hydrokinetic turbines. *Ocean Engineering*, 96:215–225, 2015. Citado 3 vezes nas páginas 53, 99, and 103.

[133] Mohammad Shahsavarifard and Eric Louis Bibeau. Yaw operation of a shrouded horizontal axis hydrokinetic turbine. In *MTS/IEEE OCEANS 2015 - Genova*, Department of Mechanical Engineering, University of Manitoba, Winnipeg, Canada, 2015. Institute of Electrical and Electronics Engineers Inc. Citado na página 53.

[134] Mohxammad Shahsavarifard and Eric Louis Bibeau. Performance characteristics of shrouded horizontal axis hydrokinetic turbines in yawed conditions. *Ocean Engineering*, 197, 2020. Citado na página 53.

[135] W Shi, D Wang, M Atlar, B Guo, and K.-C. Seo. Optimal design of a thin-wall diffuser for performance improvement of a tidal energy system for an AUV. *Ocean Engineering*, 108:1–9, 2015. Citado 3 vezes nas páginas 41, 99, and 103.

[136] M Shives and C Crawford. Ducted turbine blade optimization using numerical simulation. In *21st International Offshore and Polar Engineering Conference, ISOPE-2011*, pages 407–413, Department of Mechanical Engineering, University of Victoria, Victoria, BC, Canada, 2011. Citado na página 32.

[137] M Shives and C Crawford. Developing an empirical model for ducted tidal turbine performance using numerical simulation results. *Proceedings of the Institution of Mechanical Engineers, Part A: Journal of Power and Energy*, 226(1):112–125, 2012. Citado na página 32.

[138] Ke Song, W.-Q. Wen Quan W.-Q. Wen Quan W.-Q. Wang, and Yan Yan. Numerical and experimental analysis of a diffuser-augmented micro-hydro turbine. *Ocean Engineering*, 171(December 2018):590–602, 2019. Citado 3 vezes nas páginas 36, 98, and 102.

[139] F Sorribes-Palmer, A S Andres, A Figueroa, L Donisi, S Franchini, and M Ogueta. Aerodynamic design of a wind turbine diffuser with OpenFOAM. In *7th European and African Conference on Wind Engineering, EACWE 2017*, Instituto de Microgravedad Ignacio Da Riva, Universidad Politécnica de Madrid (IDR/UPM), Spain, 2017. International Association for Wind Engineering (IAWE). Citado na página 33.

[140] F Sorribes-Palmer, A Sanz-Andres, L Ayuso, R Sant, and S Franchini. Mixed CFD-1D wind turbine diffuser design optimization. *Renewable Energy*, 105:386–399, 2017. Citado na página 48.

[141] Huihui Sun and Yusaku Kyozuka. Analysis of performances of a shrouded horizontal axis tidal turbine. In *OCEANS 2012 MTS/IEEE Yeosu Conference: The Living Ocean and Coast - Diversity of Resources and Sustainable Activities*, Department of Earth System Science and Technology, Kyushu University, Fukuoka, Japan, 2012. Citado 2 vezes nas páginas 101 and 105.

[142] S Takahashi, Y Hata, Y Ohya, T Karasudani, and T Uchida. Behavior of the blade tip vortices of a wind turbine equipped with a brimmed-diffuser shroud. *Energies*, 5(12):5229–5242, 2012. Citado na página 37.

[143] G Tampier, C Troncoso, and F Zilic. Numerical analysis of a diffuser-augmented hydrokinetic turbine. *Ocean Engineering*, 145:138–147, 2017. Citado 3 vezes nas páginas 63, 98, and 102.

[144] P.D.C. Ten Hoopen. *An Experimental and Computational Investigation of a Diffuser Augmented Wind Turbine: with an application of vortex generators on the diffuser trailing edge*. PhD thesis, Delft University of Technology, 2009. Citado 2 vezes nas páginas 9 and 46.

[145] K Toshimitsu, K Nishikawa, W Haruki, S Oono, M Takao, and Y Ohya. PIV measurements of flows around the wind turbines with a flanged-diffuser shroud. *Journal of Thermal Science*, 17(4):375–380, 2008. Citado na página 43.

[146] Gerard J.W. W Van Bussel, Dr Gerard J W van Bussel, and Gerard J.W. W Van Bussel. The science of making more torque from wind: Diffuser experiments and theory revisited. *Journal of Physics: Conference Series*, 75(1):012010, 7 2007. Citado 2 vezes nas páginas 24 and 31.

[147] Frits F.A. van Dorst and Wind Energy. *An Improved Rotor Design for a Diffuser Augmented Wind Turbine*. PhD thesis, 2011. Citado na página 50.

[148] N. J. van Eck and L. Waltman. Software Survey: VOSviewer, a Computer Program for Bibliometric Mapping. *Scientometrics*, 84/2:523–38, 2010. Citado 3 vezes nas páginas 8, 21, and 22.

[149] J R P Vaz and D H Wood. Aerodynamic optimization of the blades of diffuser-augmented wind turbines. *Energy Conversion and Management*, 123:35–45, 2016. Citado na página 32.

[150] R Venters and B Helenbrook. A numerical investigation of high lift coefficient airfoils near regions of stall. In *ASME 2013 Fluids Engineering Division Summer Meeting, FEDSM 2013*, volume 1 A, Department of Mech. and Aero. Engineering, Clarkson University, 8 Clarkson Ave., Potsdam, NY 13699-5725, United States, 2013. Citado na página 36.

[151] C Vermillion, T Grunnagle, and I Kolmanovsky. Modeling and control design for a prototype lighter-than-air wind energy system. In *2012 American Control*

Conference, ACC 2012, pages 5813–5818, Altaeros Energies, Boston, MA 02210, United States, 2012. Citado na página 53.

[152] C Vermillion, T Grunnagle, R Lim, and I Kolmanovsky. Model-based plant design and hierarchical control of a prototype lighter-than-air wind energy system, with experimental flight test results. *IEEE Transactions on Control Systems Technology*, 22(2):531–542, 2014. Citado 2 vezes nas páginas 25 and 53.

[153] W.-Q. Wang, K Song, and Y Yan. Influence of interaction between the diffuser and rotor on energy harvesting performance of a micro-diffuser-augmented hydrokinetic turbine. *Ocean Engineering*, 189, 2019. Citado na página 33.

[154] Wen-xue Wang, Terutake Matsubara, Junfeng Hu, Satoru Odahara, Tomoyuki Nagai, Takashi Karasutani, and Y Ohya. Experimental investigation into the in fl uence of the fl anged diffuser on the dynamic behavior of CFRP blade of a shrouded wind turbine. *Renewable Energy*, 78:386–397, 2015. Citado na página 51.

[155] K Watanabe and Y Ohya. Multi-rotor systems using ducted wind turbines for power output increase (Multi lens turbine). In *AIAA Scitech Forum, 2019*, Kyushu University Platform of Inter/Transdisciplinary Energy Research, Kasugai, 816-8580, Japan, 2019. American Institute of Aeronautics and Astronautics Inc, AIAA. Citado na página 50.

[156] K Watanabe and Y Ohya. Multirotor Systems Using Three Shrouded Wind Turbines for Power Output Increase. *Journal of Energy Resources Technology, Transactions of the ASME*, 141(5), 2019. Citado na página 50.

[157] K Watanabe, Y Ohya, and T Uchida. Power output enhancement of a ducted wind turbine by stabilizing vortices around the duct. *Energies*, 12(16), 2019. Citado na página 44.

[158] S. J. Watson, D. G. Infield, J. P. Barton, and S. J. Wylie. Modelling of the performance of a building-mounted ducted wind turbine. *Journal of Physics: Conference Series*, 75(1), 2007. Citado na página 38.

[159] R Weng, K Balasubramanian, C Vermillion, and I Kolmanovsky. Model predictive longitudinal control of a lighter-than-air wind energy system. In *ASME 2012 5th Annual Dynamic Systems and Control Conference Joint with the JSME 2012 11th Motion and Vibration Conference, DSCC 2012-MOVIC 2012*, volume 2, pages 275–284, Department of Aerospace Engineering, University of Michigan, Ann Arbor, MI 48109, United States, 2012. Citado na página 53.

[160] Ben David Wood. Wind turbines augmented with rotating diffusers, February 2017. Citado na página 53.

[161] Ohya Yuji, Watanabe Koichi, Y Ohya, Watanabe Koichi, Ohya Yuji, and Watanabe Koichi. A new approach toward power output enhancement using multirotor systems with shrouded wind turbines. *Journal of Energy Resources Technology, Transactions of the ASME*, 141(5):051203, 2019. Citado na página 50.

[162] E. Zitzler and L. Thiele. Multiobjective evolutionary algorithms: A comparative case study and the strength pareto approach. *IEEE Transactions on Evolutionary Computation*, 3(4):257–271, 1999. cited By 4423. Citado na página 51.

Appendix

APPENDIX A – Database search keywords

The full set of keywords employed in the current work is presented below. The formatting is maintained in raw text without tables so the interested reader may directly copy and paste the search terms on the Scopus database using the advanced search feature. Figure A.1

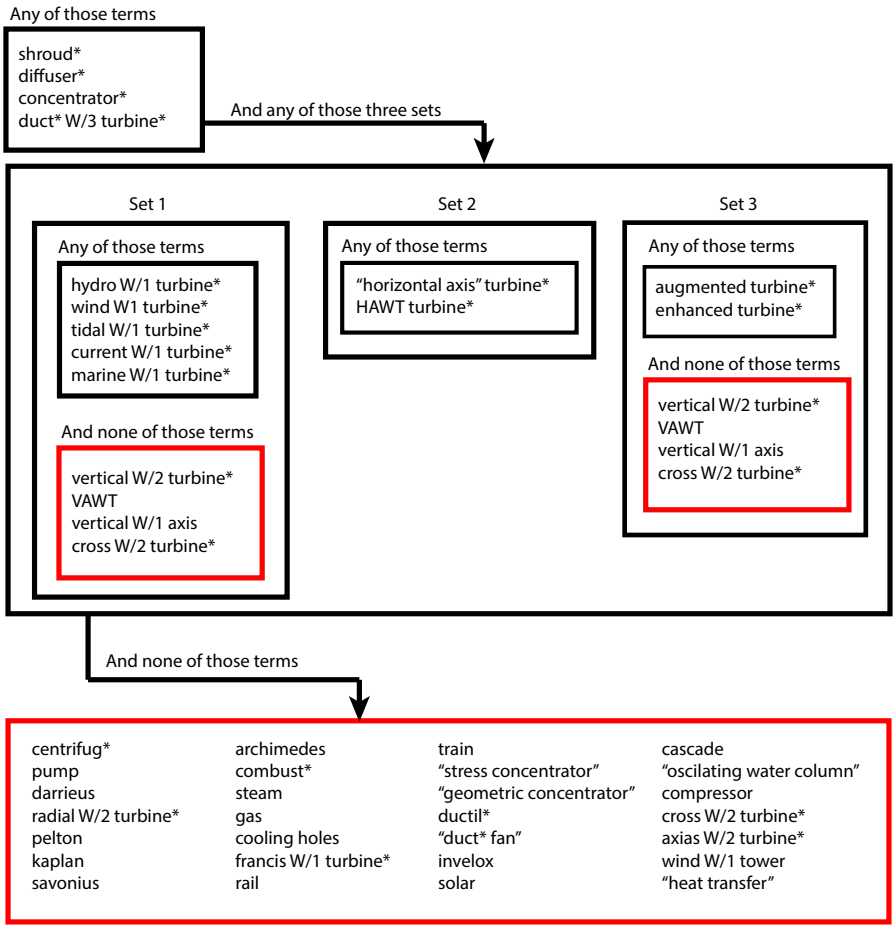

Figure A.1 – Keywords for advanced search in Scopus database.

(TITLE-ABS-KEY (shroud*) OR TITLE-ABS-KEY (diffuser*) OR TITLE-ABS-KEY (concentrator*) OR TITLE-ABS-KEY (duct* W/3 turbine*)) AND (((TITLE-ABS-KEY (hydro* W/1 turbine*) OR TITLE-ABS-KEY (wind W/1 turbine*) OR TITLE-ABS-KEY (tidal W/1 turbine*) OR TITLE-ABS-KEY (current W/1 turbine*) OR TITLE-ABS-KEY (marine W/1 turbine*)) AND NOT (TITLE-ABS-KEY (vertical W/2 turbine) OR TITLE-ABS-KEY (VAWT) OR TITLE-ABS-KEY (vertical W/1 axis) OR TITLE-ABS-KEY (cross W/2 turbine))) OR ((TITLE-ABS-KEY ("horizontal axis") OR TITLE-ABS-KEY (HAWT)) AND TITLE-ABS-KEY (turbine*)) OR ((TITLE-ABS-KEY (augmented) OR TITLE-ABS-KEY (enhanced)) AND TITLE-ABS-KEY (turbine*) AND NOT (TITLE-ABS-KEY (vertical W/2 turbine) OR TITLE-ABS-KEY (VAWT) OR TITLE-ABS-KEY (vertical W/1 axis) OR TITLE-ABS-KEY (cross W/2 turbine)))) AND NOT (TITLE-ABS-KEY (centrifug*) OR TITLE-ABS-KEY (pump) OR TITLE-ABS-KEY (darrieus) OR TITLE-ABS-KEY (radial W/2 turbine) OR TITLE-ABS-KEY (pelton) OR TITLE-ABS-KEY (kaplan) OR TITLE-ABS-KEY (savonius) OR TITLE-ABS-KEY (archimedes) OR TITLE-ABS-KEY (combust*) OR TITLE-ABS-KEY (steam) OR TITLE-ABS-KEY (gas) OR TITLE-ABS-KEY ("cooling holes") OR TITLE-ABS-KEY (francis W/1 turbine) OR TITLE-ABS-KEY (rail) OR TITLE-ABS-KEY (train) OR TITLE-ABS-KEY ("stress concentrator*") OR TITLE-ABS-KEY ("geometric concentrator*") OR TITLE-ABS-KEY (ductil*) OR TITLE-ABS-KEY ("duct* fan") OR TITLE-ABS-KEY (invelox) OR TITLE-ABS-KEY (solar) OR TITLE-ABS-KEY (cascade) OR TITLE-ABS-KEY ("oscillating water column") OR TITLE (compressor) OR TITLE (cross W/2 turbine) OR TITLE (axial W/2 turbine) OR TITLE (wind W/1 tower) OR KEY ("heat transfer")) AND (LIMIT-TO (LANGUAGE,"English"))

APPENDIX B – Diffuser-augmented turbine's data

Table B.1 – Power coefficient and tip-speed ratio data of diffuser-augmented turbines - Part I

Id.	Type	Power coefficient				Tip-speed-ratio	
		C_p^b	C_p	C_p^d	$\mathscr{E}_d$	TSR^*_{center}	TSR^*_{width}
[104]	Experimental	0.39	0.58	0.42	0.07	0.75	0.00
[104]	Experimental	0.39	0.70	0.42	0.08	0.85	-0.20
[138]	Experimental	0.42	0.67	0.38	-0.08	0.00	-0.50
[24]	Numerical	0.29	0.49	0.07	-0.76	-0.50	0.00
[96]	Experimental	0.30	0.75	0.43	0.42	0.00	0.00
[28]	Numerical	0.41	0.78	0.28	-0.32		
[28]	Numerical	0.41	0.90	0.32	-0.21		
[124]	Numerical	0.59	1.44	0.30	-0.50		
[59]	Numerical	0.37		0.57	0.54	0.38	0.25
[143]	Numerical	0.44	0.61	0.19	-0.57	0.88	0.25
[53]	Experimental	0.36	0.37	0.25	-0.29	-0.20	0.60
[53]	Experimental	0.36	0.45	0.26	-0.29	-0.38	-0.25
[115]	Experimental	0.22	0.37	0.20	-0.08	0.68	0.05
[32]	Experimental	0.39	0.76	0.44	0.14	0.25	-0.50
[31]	Experimental	0.39	0.78	0.44	0.14	-0.20	-1.00
[130]	Experimental	0.37	0.71	0.43	0.16	-0.88	-0.25

Table B.2 – Power coefficient and tip-speed ratio data of diffuser-augmented turbines - Part II

Id.	Type	Power coefficient				Tip-speed-ratio	
		C_p^b	C_p	C_p^d	$\mathscr{E}_d$	TSR^*_{center}	TSR^*_{width}
[83]	Experimental	0.11		0.23	1.05	0.43	-0.05
[135]	Experimental	0.42	0.70	0.25	-0.40	0.73	-1.25
[135]	Experimental	0.42	0.82	0.30	-0.30	1.53	-0.85
[132]	Experimental	0.38	0.54	0.34	-0.11	-0.05	-0.50
[132]	Experimental	0.38	0.71	0.45	0.17	0.43	-0.55
[126]	Numerical	0.32	0.48	0.22	-0.32	1.20	0.40
[127]	Experimental	0.42	0.59	0.33	-0.21	0.85	-0.50
[127]	Experimental	0.42	0.68	0.26	-0.38	0.75	-0.70
[113]	Experimental			0.62			
[113]	Numerical		0.99	0.57			
[113]	Numerical		1.05	0.59			
[26]	Experimental	0.43	0.93	0.32	-0.26	1.43	0.05
[108]	Experimental		0.74			0.68	0.15
[82]	Experimental	0.26		0.41	0.58	0.68	0.15
[82]	Experimental	0.26		0.43	0.63	0.73	0.05
[82]	Experimental	0.26		0.46	0.77	1.13	0.05
[82]	Experimental	0.26		0.43	0.65	1.45	0.10
[82]	Experimental	0.26		0.44	0.69	0.75	0.70
[82]	Experimental	0.26		0.44	0.69	1.55	0.30
[82]	Experimental	0.26		0.52	1.00	0.55	-0.20
[27]	Experimental	0.22	0.45	0.23	0.06	0.50	0.00

Table B.3 – Power coefficient and tip-speed ratio data of diffuser-augmented turbines - Part III

Id.	Type	Power coefficient				Tip-speed-ratio	
		C_p^b	C_p	C_p^d	$\mathscr{E}_d$	TSR^*_{center}	TSR^*_{width}
[27]	Experimental	0.24	0.58	0.30	0.26	0.28	-0.15
[27]	Experimental	0.32	0.64	0.33	0.04	0.43	-0.05
[27]	Experimental	0.36	0.66	0.34	-0.05		
[27]	Experimental		0.61	0.32			
[27]	Experimental		0.67	0.35		-0.40	-0.20
[105]	Experimental	0.37	0.77	0.45	0.22	-0.15	-0.30
[105]	Experimental	0.37	0.88	0.47	0.28	-0.30	0.00
[105]	Experimental	0.37	0.88	0.47	0.28	-0.35	-0.10
[105]	Experimental	0.37	0.70	0.43	0.15	0.00	0.00
[105]	Experimental	0.37	0.74	0.44	0.20	-0.08	-0.35
[105]	Experimental	0.37	0.79	0.45	0.23	0.25	-0.10
[105]	Experimental	0.37	0.91	0.42	0.13		
[105]	Experimental	0.37	0.70	0.49	0.34		
[105]	Experimental	0.37	0.77	0.40	0.07		
[105]	Experimental	0.37	0.79	0.35	-0.05		
[105]	Experimental	0.37	0.75	0.51	0.37		
[105]	Experimental	0.37	0.83	0.41	0.11		
[105]	Experimental	0.37	0.85	0.37	-0.01		
[105]	Experimental	0.37	0.78	0.49	0.32		
[105]	Experimental	0.37	0.95	0.44	0.19		
[105]	Experimental	0.37	0.97	0.39	0.07		

Table B.4 – Power coefficient and tip-speed ratio data of diffuser-augmented turbines - Part IV

Id.	Type	Power coefficient				Tip-speed-ratio	
		C_p^b	C_p	C_p^d	$\mathscr{E}_d$	TSR^*_{center}	TSR^*_{width}
[105]	Experimental	0.37	0.81	0.43	0.16		
[105]	Experimental	0.37	0.96	0.39	0.04		
[105]	Experimental	0.37	1.02	0.36	-0.02	1.28	-0.05
[3]	Experimental	0.26	1.15	0.17	-0.34	0.85	-0.30
[141]	Experimental	0.36	0.88	0.46	0.29		
[78]	Numerical		0.82	0.47			
[78]	Numerical		0.95	0.45			
[78]	Numerical		0.83	0.48			
[78]	Numerical		0.92	0.50		1.35	0.10
[120]	Numerical	0.32	1.45				
[57]	Numerical		0.72	0.27		-0.35	-0.30
[47]	Numerical	0.44	0.95	0.32	-0.28	-0.75	-0.50
[47]	Numerical	0.44	1.13	0.28	-0.36	-0.60	-0.80
[47]	Numerical	0.44	1.20	0.24	-0.45	-0.75	-1.10
[47]	Numerical	0.44	1.25	0.21	-0.53		

APPENDIX C – Diffuser-augmented turbine's geometry

Table C.1 – Geometry data of diffuser-augmented turbines - Part I

Id.	Type	Geometry					
		D_r [mm]	D_i [mm]	D_d [mm]	A_d/A_r	θ [°]	L [mm]
[104]	Experimental	224	246	264	1.39	10	49
[104]	Experimental	224	240	289	1.66		49
[138]	Experimental	500		661	1.75		250
[24]	Numerical	800	1772	4243	28.13		2053
[96]	Experimental	1190	1181	1578	1.76	15	739
[28]	Numerical	1360	1496	2281	2.81		680
[28]	Numerical	1360	1496	2281	2.81		680
[124]	Numerical	200		440	4.84		300
[59]	Numerical	1160	1262	1609	1.92		261
[143]	Numerical	2000	2382	3605	3.25		2282
[53]	Experimental	265	288	318	1.43		
[53]	Experimental	265	282	352	1.76		
[115]	Experimental	320	335	437	1.86		335
[32]	Experimental						
[31]	Experimental	612	620	812	1.76	26	180
[130]	Experimental		620				

Table C.2 – Geometry data of diffuser-augmented turbines - Part II

Id.	Type	Geometry					
		D_r [mm]	D_i [mm]	D_d [mm]	A_d/A_r	θ [°]	L [mm]
[83]	Experimental	190	195	249	1.72	12	120
[135]	Experimental	300	302	500	2.78		220
[135]	Experimental	300	302	500	2.78		220
[132]	Experimental	198	226	250	1.59	25	77
[132]	Experimental	198	201	250	1.59	25	52
[126]	Numerical	457	457	677	2.19	4	914
[127]	Experimental	533	610	711	1.78		152
[127]	Experimental	533	610	864	2.63		152
[113]	Experimental	1000		1269	1.61		211
[113]	Numerical	1000					263
[113]	Numerical	1000					263
[26]	Experimental	400	440	684	2.92	4	706
[108]	Experimental						
[82]	Experimental	190	195	241	1.61	12	120
[82]	Experimental	190		241	1.61	12	
[82]	Experimental	190	195	269	2.00	11	186
[82]	Experimental	190	195	289	2.31	11	232
[82]	Experimental	190	195	309	2.64	12	279
[82]	Experimental	190	195	283	2.22	12	120
[82]	Experimental	190	195	327	2.96	12	120
[27]	Experimental	300	300	416	1.92	30	100

Table C.3 – Geometry data of diffuser-augmented turbines - Part III

Id.	Type	Geometry					
		D_r [mm]	D_i [mm]	D_d [mm]	A_d/A_r	θ [°]	L [mm]
[27]	Experimental	300	300	416	1.92	30	100
[27]	Experimental	300	300	416	1.92	30	100
[27]	Experimental	300	300	416	1.92	30	100
[27]	Experimental	300	300	416	1.92	30	100
[27]	Experimental	300	300	416	1.92	30	100
[105]	Experimental	1000	1120	1309	1.71		230
[105]	Experimental	1000	1080	1362	1.85		225
[105]	Experimental	1000	1120	1364	1.86		225
[105]	Experimental	1000	1080	1283	1.65	12	230
[105]	Experimental	1000		1292	1.67		102
[105]	Experimental	1000		1318	1.74		140
[105]	Experimental	1000		1476	2.18		378
[105]	Experimental	1000		1190	1.42		102
[105]	Experimental	1000		1394	1.94		102
[105]	Experimental	1000		1496	2.24		102
[105]	Experimental	1000		1216	1.48		140
[105]	Experimental	1000		1420	2.02		140
[105]	Experimental	1000		1522	2.32		140
[105]	Experimental	1000	1120	1262	1.59		225
[105]	Experimental	1000	1120	1466	2.15		225
[105]	Experimental	1000	1120	1568	2.46		225

Table C.4 – Geometry data of diffuser-augmented turbines - Part IV

Id.	Type	Geometry					
		D_r [mm]	D_i [mm]	D_d [mm]	A_d/A_r	θ [°]	L [mm]
[105]	Experimental	1000		1374	1.89		378
[105]	Experimental	1000		1578	2.49		378
[105]	Experimental	1000		1680	2.82		378
[3]	Experimental	388	456	1013	6.81	12	617
[141]	Experimental	300		413	1.89		68
[78]	Numerical	1000	1088	1314	1.73		185
[78]	Numerical	1000	1116	1452	2.11		295
[78]	Numerical	1000	1096	1316	1.73		253
[78]	Numerical	1000	1072	1360	1.85		300
[120]	Numerical	457					
[57]	Numerical	3000	4900	4370	2.67		
[47]	Numerical				3.00		
[47]	Numerical				4.00		
[47]	Numerical				5.00		
[47]	Numerical				6.00		